Comparison of three aerosol chemical characterization techniques utilizing PTR-ToF-MS: A study on freshly formed and aged biogenic SOA

Giorgos I. Gkatzelis [1], Ralf Tillmann[1], Thorsten Hohaus [1], Markus Müller [2,4], Philipp Eichler [2†], Kang-Ming Xu [3], Patrick Schlag [1††], Sebastian H. Schmitt [1], Robert Wegener[1], Martin Kaminski[1], Rupert Holzinger [3], Armin Wisthaler [2,5], Astrid Kiendler-Scharr [1]

[1] Institute of Energy and Climate Research, IEK-8: Troposphere, Forschungszentrum Jülich GmbH, Jülich, Germany
[2] Institut für Ionenphysik und Angewandte Physik, Universität Innsbruck, Innsbruck, Austria
[3] Institute for Marine and Atmospheric research Utrecht, Princetonplein 5, 3584 CC, Utrecht, The Netherlands
[4] Ionicon Analytik GmbH, Innsbruck, Austria
[5] Department of Chemistry, University of Oslo, Norway

[†]Now at: German Environment Agency, Dessau-Roßlau, Germany

[††]Now at: Institute of Physics, University of Sao Paulo, Sao Paulo, Brazil

Correspondence to: R. Tillmann (r.tillmann@fz-juelich.de)

Abstract

An inter-comparison of different aerosol chemical characterization techniques has been performed as part of a chamber study of biogenic SOA formation and aging at the atmosphere simulation chamber SAPHIR. Three different aerosol sampling techniques, the aerosol collection module (ACM), the chemical analysis of aerosol on-line (CHARON) and the collection thermal desorption unit (TD) were connected to Proton Transfer Reaction Time of Flight Mass Spectrometers (PTR-ToF-MS) to provide chemical characterization of the SOA. The techniques were compared among each other and to results from an Aerosol Mass Spectrometer (AMS) and a Scanning Mobility Particle Sizer (SMPS). The experiments investigated SOA formation from the ozonolysis of β-pinene, limonene, a β-pinene/limonene mix and real plant emissions from *Pinus sylvestris L.* (Scots pine). The SOA was subsequently aged by photooxidation except for limonene SOA which was aged by NO_3 oxidation.

Despite significant differences in the aerosol collection and desorption methods of the PTR based techniques, the determined chemical composition, i.e. the same major contributing signals were found by all instruments for the different chemical systems studied. These signals could be attributed to known products expected from the oxidation of the examined monoterpenes. The sampling and desorption method of ACM and TD, provided additional information on the volatility of individual compounds and showed relatively good agreement.

Averaged over all experiments, the total aerosol mass recovery compared to an SMPS varied from 80 ± 10%, 51 ± 5% and 27 ± 3% for CHARON, ACM and TD, respectively. Comparison to the oxygen to carbon ratios (O:C) obtained by AMS showed that all PTR based techniques observed lower O:C ratios indicating a loss of molecular oxygen either during aerosol sampling or detection. The differences in total mass recovery and O:C between the three instruments resulted predominantly from differences in the field strength (E/N) in the drift-tube reaction ionization chambers of the PTR-ToF-MS instruments and from dissimilarities in the collection/desorption of

aerosols. Laboratory case studies showed that PTR-ToF-MS E/N conditions influenced fragmentation which resulted in water and further neutral fragment losses of the detected molecules. Since ACM and TD were operated in higher E/N compared to CHARON this resulted to higher fragmentation, thus affecting primarily the detected oxygen and carbon content and therefore also the mass recovery. Overall, these techniques have been shown to provide valuable insight on the chemical characteristics of BSOA, and can address unknown thermodynamic properties such as partitioning coefficient values and volatility patterns down to a compound specific level.

1 Introduction

Atmospheric organic aerosols (OA) represent a major contribution to the submicrometer particulate matter (PM_1) thus playing a key role in climate change and air quality (Kanakidou et al., 2005). OA are either directly emitted through e.g. combustion processes (primary OA, POA) or formed through the oxidation of volatile organic compounds (VOCs), called secondary OA (SOA) (Seinfeld and Pandis, 2006). SOA constitute a major fraction of OA (Jimenez et al., 2009) with biogenic VOC oxidation products affecting their global contribution (Guenther et al., 2012). Due to thousands of individual compounds involved in SOA, the chemical characterization of OA still presents a huge analytical challenge (Goldstein and Galbally, 2007). The ability of these compounds to condense to the particulate-phase or partition between the gas and particle phase as well as their volatility are thermodynamic parameters of interest that determine their atmospheric fate.

Various techniques have been established in order to better quantify and chemically characterize SOA (Hallquist et al., 2009). These techniques optimize and compromise for time, size or chemical resolution combined with the percentage of OA mass they can detect. Off-line techniques, based on filter measurement, provide detailed information on functional groups or individual chemical species while having low time resolution (hours to days) and size information. On-line techniques, like e.g. the Aerodyne aerosol mass spectrometer (AMS) (Canagaratna et al., 2007), provide high time resolution and size resolved data while less specific chemical composition information or molecular identification of the OA compounds is acquired.

In recent years attempts to develop new techniques that combine both chemical identification but also improved time resolution have been established. These techniques use different pre-concentration methods in order to detect the particulate-phase compounds. Filter based techniques like the Filter Inlet for Gases and AEROsols (FIGAERO) (Lopez-Hilfiker et al., 2014) provide highly effective collection of particles on filters, under high flow rates (30 standard Liters per minute, sLpm), thus low collection times. Thermal desorption of the sampled particles on the filter is performed with the disadvantage of sampling artefacts from gas-phase compounds that may condense on the large surface area of the filter and contribute to the overall signal. Other techniques, like the thermal desorption aerosol gas chromatograph (TAG) (Kreisberg et al., 2009; Williams et al., 2006) or the collection thermal desorption unit (TD) (Holzinger et al., 2010b), utilize the concept of particle collection on an impaction surface by means of humidification and inertial impaction, followed by desorption. TAG and TD provide hourly time resolution measurements, and when combined with a gas-phase denuder avoid sampling of additional gas-phase constituents on their collection thermal desorption (CTD) cell. Due to the particle humidification step these techniques may bias collection efficiency towards water soluble compounds. The aerosol collection module (ACM)

(Hohaus et al., 2010) collects aerosols by passing them through an aerodynamic lens for particle collimation (Liu et al., 1995a; b), further through a vacuum system (comparable in design to the AMS), and finally impacting the particle phase on a cooled sampling surface. Although the ACM has a low time resolution (3-4 h), it's design makes it applicable for the investigation of compound specific thermodynamic properties e.g. partitioning coefficient and volatility (Hohaus et al., 2015). The chemical analysis of aerosol online (CHARON) (Eichler et al., 2015) is a technique that provides on-line real time measurements by passing the particles through a denuder to strip off the gas-phase. Particles are sampled through an aerodynamic lens combined with an inertial sampler for the particle-enriched flow, and a thermodesorption unit for particle volatilization prior to chemical analysis. The enrichment factor of this system is known by performing calibrations, thus reducing the quantification uncertainty. All the above pre-concentration systems detect the compounds originating from the particulate-phase that underwent evaporation to the gas-phase by desorption, thus introducing possible thermal break down of analytes.

A variety of detection instruments have been coupled to these inlet techniques, providing different functionality and chemical composition information. The proton transfer reaction time of flight mass spectrometer (PTR-ToF-MS) (Jordan et al., 2009) is a soft ionization technique with low detection limits and high time resolution (ms), that can cover a wide volatility range, from VOCs to low-volatility VOCs (LVOCs), depending on the inlet used (Eichler et al., 2017). Techniques utilizing a PTR-ToF-MS are capable of measuring a large fraction of the OA mass, ranging from 20 to 100% (Eichler et al., 2015; Mensah et al., 2012), and provide additional information on the elemental composition of the organic compounds; however, the compound's molecular identity attribution is challenging. On the contrary, gas chromatography mass spectrometry is considered ideal for detailed compound specific structural analysis. Techniques like the TAG have been applied utilizing a gas chromatograph, to provide non-polar and low-polarity tracers identification while the modified semi-volatile TAG (SV-TAG) has broadened this range to highly polar oxygenates, mostly seen in the atmosphere, by using online derivatization (Isaacman et al., 2014; Zhao et al., 2013). The volatility and polarity separator (VAPS) is a similar technique that provides volatility- and polarity-resolved OA information by using a modified 2-dimensional gas chromatography (2D-GC) approach combined with high resolution time -of -flight mass spectrometry (Martinez et al., 2016). Although these techniques provide chemical speciation and lower time resolution, they can only do so for a small fraction of the OA mass (10 - 40%).

The specificity of the above newly developed techniques is still to be explored in detail. In this work, an inter-comparison campaign was performed in the atmosphere simulation chamber SAPHIR (Rohrer et al., 2005) to investigate biogenic SOA (BSOA) formation and aging. The focus of this work is on the comparison of three different aerosol characterization techniques, the ACM - PTR-ToF-MS, the TD - PTR-ToF-MS and the CHARON - PTR-ToF-MS. The OA mass fraction these techniques were able to detect combined with the OA chemical characteristics and volatility trends were investigated and compared.

2 Methods and instrumentation

2.1 Facilities

Experiments were conducted in the atmospheric simulation chamber SAPHIR (Simulation of Atmospheric PHotochemistry In a large Reaction chamber) located in Jülich, Germany. The chamber consisted of twin FEP

Teflon foils with a volume of 270 m^3, resulting in a surface to volume ratio of approximately 1 m^{-1}. High purity nitrogen (99.9999% purity) was flushed at all times to the space between the twin walls and a pressure gradient was maintained in order to prevent contamination from outside. A high flow (150 to 200 m^3 h^{-1}) of air was introduced in order to clean the chamber and reach aerosol and trace gases concentrations below detection limits before each experiment was initiated. A low flow (8 m^3 h^{-1}) was used to replenish SAPHIR during experiments from losses due to leaks and sampling of the instruments. The chamber is equipped with a louvre system thus experiments could be performed under dark conditions focusing on O_3 and NO_3 oxidation (roof closed) or as photooxidation experiments utilizing sun light (roof open). More details on SAPHIR can be found in Rohrer et al. (2005).

A PLant chamber Unit for Simulation (PLUS) was recently coupled to SAPHIR to investigate the impact of real plant emissions on atmospheric chemistry (Hohaus et al., 2016). PLUS is an environmentally controlled, flow through plant chamber where continuous measurements and adjustments of important environmental parameters (e.g., soil relative humidity, temperature, photosynthetical active radiation) are performed. To simulate solar radiation and control the tree emissions in PLUS, 15 light-emitting diode (LED) panels were used with an average photosynthetically active radiation value (PAR) of 750 nm and an average temperature of 25 °C . In this study, BVOC emissions were generated from 6 *Pinus sylvestris L*. (Scots pine) trees.

A set of standard instrumentation was coupled to the simulation chamber SAPHIR. Air temperature was measured by an ultrasonic anemometer (Metek USA-1, accuracy 0.3 K) and humidity was determined with a frost point hygrometer (General Eastern model Hygro M4). NO and NO_2 measurements were performed with a chemiluminescence analyser (ECO PHYSICS TR480) equipped with a photolytic converter (ECO PHYSICS PLC760). Ozone was measured by an UV absorption spectrometer (ANSYCO model O341M). Particle size distribution was measured using a Scanning Mobility Particle Analyser (SMPS TSI, TSI Classifier model 3080, TSI DMA 3081, TSI Water CPC 3786), measuring in the 10 - 450 nm range with a time resolution of 8.5 min and an accuracy of 12% (Wiedensohler et al., 2012). A High-Resolution Time-of-Flight Aerosol Mass Spectrometer (HR-ToF-AMS) (Canagaratna et al., 2007; DeCarlo et al., 2006) was used to determine the total organic mass and composition of the SOA formed with an accuracy of 31% (Aiken et al., 2008). High resolution mass spectra were analyzed using the software packages SQUIRREL (v1.57) and PIKA (v1.15Z). Oxygen to carbon ratios were calculated based on the newly developed "Improved-Ambient" method by Canagaratna et al. (2015).

2.2 Experimental procedure

SOA was formed through the ozonolysis of different monoterpenes using the simulation chamber SAPHIR. Experimental starting conditions varied from the injection of β-pinene and limonene, as single compounds or as a mixture, to the injection of real plant emissions from 6 Pinus sylvestris *L*. (Scots pine), provided from SAPHIR-PLUS (Section 2.1). For the tree emissions experiment the BVOCs consisted of 42% δ^3-carene, 38% α-pinene, 5% β-pinene, 4% myrcene, 3% terpinolene and 8% other monoterpenes, as determined by GC-MS measurements. The details of the experiments are given in Table 1. The chamber was initially humidified (55% RH, 295 – 310 K) and background measurements for all instruments were performed. Monoterpenes were injected either with a Hamilton syringe injection and subsequent evaporation into the replenishment flow of SAPHIR, or by SAPHIR-PLUS (real

tree emissions). After one hour, ozone was introduced in the system to initiate chemistry. The ozonolysis of monoterpenes and the tree emissions was performed under low NO_x conditions (10 – 60 pptV) in the absence of an OH scavenger. For the limonene experiment, 8 hours after the ozone injection, an addition of 30 ppbV of NO was introduced into the dark chamber. The reaction of NO_2 with remaining ozone in the dark chamber resulted in the generation of NO_3, thus initiating the NO_3 oxidation chemistry. In all other experiments the chamber was illuminated 20 hours after the ozone injection, exposing the SOA to real sunlight, thus initiating photo-oxidation by OH radicals. Finally, for the real tree emissions, after 11 hours of ozone exposure, additional biogenic VOCs (BVOCs) were re-introduced into the SAPHIR chamber to generate fresh SOA which was subsequently aged by photooxidation for additional 6 hours. The duration of the experiments varied from 17 to 36 hours, providing ample time to experimentally investigate the aging of the biogenic SOA.

2.3 PTR-ToF-MS aerosol chemical characterization techniques

Three independent aerosol chemical characterization techniques utilizing PTR-ToF-MS were compared, the aerosol collection module (ACM – PTR-ToF-MS, referred to as "ACM" hereafter), the chemical analysis of aerosol online (CHARON – PTR-ToF-MS, referred to as "CHARON" hereafter) and the collection thermal desorption unit (TD – PTR-ToF-MS, referred to as "TD" hereafter). Their characteristics and differences are provided in Table 2 and discussed in detail in this section. The time resolution of the techniques varied from CHARON providing online measurements to the TD and ACM having increased collection times of 30 and 240 min, respectively. CHARON was operated at a constant temperature and lower pressure (< 1 atm) while ACM and TD, operated at 1 atm, introduced temperature ramps during desorption thus providing more detailed volatility information. The pre-concentration factor for ACM and TD was calculated from the ratio of the volume sampled during collection to the volume evaporated during desorption, assuming a 3 min desorption time for an individual compound. The limit of detection (LOD), dependent on the different pre-concentration factors for each technique, resulted in TD having the lowest LOD (0.02 ng m^{-3}), followed by the CHARON (1.4 ng m^{-3}), while ACM showed the highest values (35 ng m^{-3}). It should be noted that for the individual PTRMS the LOD for gas-phase measurements, bypassing any pre-concentration step, agreed within a factor of two. Different electric field strength (V cm^{-1}) to buffer gas density (molecules cm^{-3}) ratio (E/N) conditions were applied to the PTR-ToF-MS of each aerosol chemical characterization technique. Lower E/N set values resulted in longer ion residence times in the drift tube of the PTR-ToF-MS thus higher sensitivity due to enhanced proton transfer reaction times. Ions were introduced to a lower kinetic energy system, thus resulting in reduced fragmentation during ionization while the cluster ion distribution was changed when lowering the E/N, supporting more $H_3O^+(H_2O)_n$ (n=1,2,3..) cluster ion generation (de Gouw and Warneke, 2007). Since the proton affinity of $H_3O^+(H_2O)_n$ is higher than that of H_3O^+, a certain range of organic compounds could not be ionized in such operating conditions. An overview of the primary ion distribution is provided in Figure S 1. Normalization of the signal was performed based on the sum of $500 * H_3O^+ + 250 * H_3O^+(H_2O)$ for all PTRMS. ACM and TD showed more than 98 % of the primary ions originating from H_3O^+ while for CHARON, when operated at 100 Td (1 Td = 10^{-17} V cm^{-2} $molecule^{-1}$), around 65%

originated from H_3O^+ and 35% from $H_3O^+(H_2O)$, and for CHARON at 65 Td, around 20% from H_3O^+ and 75% from $H_3O^+(H_2O)$. Based on the uncertainty in the reaction rate coefficient of the organic compounds with H_3O^+ the PTR-ToF-MS was assumed to introduce a ± 40% uncertainty on the volume mixing ratios of uncalibrated compounds for CHARON and TD. The ACM used an average sensitivity of 15 ncps/ppbV with an uncertainty of ± 50% (± 1σ) where ncps accounted for the normalized to the primary ions signal.

All PTR-ToF-MS used in this campaign were of the model PTR-TOF 8000, manufactured from Ionicon Analytik GmbH, Innsbruck, Austria. Although being the same models, minor differences in the design e.g. the TOF interface existed, related mostly to ACM when compared to CHARON and TD. These differences introduced additional fragmentation and affected the resolution of the PTRMS as reflected from Table 2. Nevertheless, the sensitivity of all PTRMS when using acetone as a calibration compound was in a similar range as observed in Figure S1. When calculating the sensitivity using the cps instead of the ncps, observed differences suggested lower primary ion signal and reaction times for ACM and TD when compared to CHARON. In the following subsections the principle of operation and operating conditions of the different inlets and PTRMS systems used in this study is reported.

2.3.1 ACM – PTR-ToF-MS

The ACM is an aerosol collection inlet with subsequent sample evaporation coupled to a gas-phase detector designed for in situ, compound specific chemical analysis. The ACM can be adapted to work with different gas-phase analysers and has previously been used coupled to a GC-MS (Hohaus et al., 2010). In this work, the ACM was coupled to a PTR-ToF-MS (model PTR-TOF 8000; Ionicon Analytik GmbH, Innsbruck, Austria).

In brief, ambient air was sampled through an aerodynamic lens (Liu et al., 1995a; b) with a flow rate of 80 ml min^{-1}. Within the aerodynamic lens the gas and particle phase of an aerosol were separated and the particles were collimated into a narrow beam. The particle beam was directed through a high vacuum environment (10^{-5} torr) to a cooled (-5 °C) sampling surface made of Siltek®/Sulfinert®-treated stainless steel. After collection was completed (a collection time of 4 h was used in this study) the particles were thermally desorbed by heating up the collector. The evaporated compounds were transferred to the PTR-ToF-MS through a coated stainless steel line of 0.8 mm inner diameter and 30 cm length, constantly kept at 300 °C. Nitrogen was used as carrier gas with a flow of 300 ml min^{-1}, resulting in a residence time of 60 ms. For this study, the collector temperature was ramped by 100 °C min^{-1} to a maximum of 250 °C, with 3-minute isothermal sections at 100 °C, 150 °C and 250 °C, respectively. During the final temperature step of 250 °C, desorption time was extended for additional 7 minutes to ensure complete evaporation of the sample. These temperature steps provided enough time for compounds to undergo evaporation within a defined volatility range. The signal dropped close to zero before each temperature step was completed, making the ACM-PTR-ToF-MS ideal for compound specific volatility trend analysis. Parallel to the ACM particulate-phase collection, a bypass line was used, coupled to the same PTR-ToF-MS, measuring the gas-phase during particle phase sampling time. An example of the gas and particulate-phase measurements is given in Figure S2. During the campaign, the aerosol-phase sampling line was a stainless steel line (total length: 4 m, OD: 1/4') with a flow of 0.7 L min^{-1}.

Assuming a collection efficiency of 100% (Hohaus et al., 2010) for all particles in the aerosol sample, measured PTR-ToF-MS signals could be converted to particulate mass concentrations by applying PTR calibrations as described in the following. Normalization of the PTR-ToF-MS counts per second was performed based on the H_3O^+ signal, resulting in ncps. The ACM was corrected for mass discrimination. The mass discrimination function was determined based on the ratio of the measured over the theoretical sensitivity of acetaldehyde, acetone, butanone, benzene, toluene, xylene and mesitelyne. The instrument was calibrated for a total of 15 compounds including aromatics (benzene, toluene, xylene, chlorobenzene), oxygenates (acetaldehyde, acetone, 2-butanone, 3-pentanone, MVK, nopinone, methanol, 1-butanol), pure hydrocarbons (isoprene, α-pinene) and acetonitrile. Calibration was performed by coupling the PTR-ToF-MS to a calibration unit (LCU, Ionicon Analytik GmbH, Innsbruck, Austria) and measuring known concentration of the compounds in the gas-phase. For signals observed at uncalibrated masses the average sensitivity of acetaldehyde, acetone, MVK, Butanon, pentanone and nopinone was applied resulting in 15 ncps/ppb. The mass concentration of an aerosol compound z_i in the air sample was calculated based on the mixing ratios the PTR-MS measures:

$$\mathbf{mz_{i,(\mu g/m^3)}} = \frac{\mathbf{mz_{i,(ppb)} \times MW_i}}{\mathbf{T \times R}} \times \frac{\mathbf{F_{N_2} \times t_{meas}}}{\mathbf{F_{col} \times t_{col}}}, \quad \textbf{(1)}$$

where $mz_{i,(\mu g/m^3)}$ is the aerosol concentration of compound i in $\mu g\, m^{-3}$, $mz_{i,(ppb)}$ the background corrected arithmetic mean of the mixing ratio during the aerosol analysis in the nitrogen flow in ppb, MW_i is the molecular weight of compound i in $gmol^{-1} -$, R is the universal gas law constant, T the ambient temperature of the SAPHIR chamber in Kelvin, F_{N_2} the flow of the carrier gas in standard liter per minute, t_{meas} the aerosol desorption duration, F_{col} the collection flow rate of the aerosol to the ACM in standard liter per minute and t_{col} the aerosol collection duration. The volume ratio correction $\left(\frac{F_{N_2} \times t_{meas}}{F_{col} \times t_{col}}\right)$ was applied in order to account for the ACM collection preconcentration step. The mass concentration was calculated by taking into account only the signal above the instrument noise (> 2σ) for each compound at each desorption.

Background measurements were performed before and after every experiment (~ 2 times per day) by heating up the collector, without depositing particles on the surface beforehand. The signal derived from the background measurements at each temperature step was then interpolated and subtracted from all desorptions for all compounds. Two major factors could affect the background signal, gas-phase interference and aerosol residual remaining at the collector after each desorption cycle. Due to the aerodynamic lens set-up the ACM design prevents gas-phase contamination (removal > 99.9999%). Background measurements throughout this study show no residual compounds on the collector in the desorption temperature range studied.

PTR-ToF-MS operation conditions were kept constant throughout the campaign. It was operated at E/N = 120 Td. The drift tube was kept at a temperature of 100 °C and a pressure of 2.30 mbar. The mass resolving power of this PTR-ToF-MS was m/Δm ~ 2500 (Δm is full width at half maximum). Mass spectra were collected up to *m/z* 400 at 10 s signal integration time. Analysis of the raw data was performed using the PTR-TOF Data Analyzer (version 4.40) software (Müller et al., 2013). In brief, an integration time of 90 s was chosen for the software and *m/z* calibration peaks were assigned based on the peaks of 21.02, 59.05 and 180.94 accounting for $H_3[18O]^+$, protonated

acetone and trichlorobenzene respectively. Trichlorobenzene was used as an internal standard throughout the campaign. The chemical composition assignment was derived from the measured exact mass assuming a molecular formula of $C_xH_yO_zN_a$ and attributing the isotopic pattern when possible.

2.3.2 CHARON – PTR-ToF-MS

The analyzer deployed by the University of Innsbruck consisted of a Chemical Analysis of Aerosol Online (CHARON) inlet interfaced to a PTR-ToF-MS.

The CHARON inlet (Eichler et al., 2015) consists of a gas-phase denuder for stripping off gas-phase analytes, an aerodynamic lens for particle collimation combined with an inertial sampler for the particle-enriched flow, and a thermodesorption unit for particle volatilization prior to chemical analysis. The monolithic charcoal denuder (Mast Carbon International Ltd., Guilford, UK) used in this study was 25 cm long, had an outer diameter of 3 cm and a channel density of 585 channels per inch (cpi). The thermodesorption unit consisted of a heated Siltek®/Sulfinert®-treated stainless steel tube kept at a temperature of 140 °C and a pressure on the order of a few mbar. A HEPA filter (ETA filter model HC01-5N-B, Aerocolloid LLC, Minneapolis, MN, USA) was periodically placed upstream of the gas-phase denuder for determining the instrumental background. More details on the performance of the CHARON inlet are given in Eichler et al. (2015).

The CHARON inlet was interfaced to a commercial PTR-ToF-MS instrument (model PTR-TOF 8000; Ionicon Analytik GmbH, Innsbruck, Austria). PTR-ToF-MS mass spectra were collected up to *m/z* 500 at 10 s signal integration time. The PTR-TOF Data Analyzer (version 4.40) software was used for data analysis (Müller et al., 2013). During the tree emissions experiment the electric field applied to the drift tube was periodically switched in 300 s intervals, i.e. measurements were performed at alternating E/N-values of 65 Td (referred to as "$CHARON_{65}$" hereafter) and 100 Td (referred to as "$CHARON_{100}$" hereafter), respectively (1 Td = 10^{-17} V cm^{-2} $molecule^{-1}$). For all other experiments the E/N-value analysed was at 100 Td. The drift tube was kept at a temperature of 120 °C and a pressure of 2.40 mbar. Continuous permeation of 1,2-diiodobenzene was performed into the drift tube for generating mass axis calibration signals at *m/z* 203.943 and *m/z* 330.847. The PTR-ToF-MS was characterized using a 16-compound gas mixture that included aromatics (benzene, toluene, o-xylene, mesitylene, chlorobenzene), oxygenate compounds (acetaldehyde, acetone, 2-butanone, 3-pentanone, MVK, nopinone, methanol, 1-butanol), pure hydrocarbons (isoprene, α-pinene) and acetonitrile. The mass resolving power of this PTR-ToF-MS was m/Δm 4500-5000.

The entire CHARON setup was calibrated using size-selected ammonium nitrate particles as described in Eichler et al. (2015). A sensitivity model based on Su and Chesnavich's parameterized reaction rate theory and a chemical composition based parameterization of polarizabilities at a constant dipole moment of μ_D = 2.75 D (between 1 – 4.5 D for most oxygenated organic compounds) was applied to calculate sensitivities of unknown compounds. This resulted in an *m/z* independent sensitivity accuracy of about ± 25%. For compounds without assigned elemental composition the polarizability of acetone was applied with an accuracy of ± 40%. Derived volume mixing ratios were transformed to mass concentrations using the molecular *m/z* information at Normal Temperature and Pressure (NTP) conditions (293.15 K, 101.325 kPa). Quantification was hampered by two events (power failure, partial

obstruction of the aerodynamic lens) which resulted in a higher than usual variability of the particle enrichment in the aerodynamic lens. Results from two experiments (limonene ozonolysis/NO_3 oxidation and limonene/β-pinene mixture ozonolysis) were particularly affected as will be shown and discussed in section 3.

The CHARON-PTR-ToF-MS setup was interfaced to the SAPHIR chamber using Siltek®/Sulfinert®-treated stainless steel tubing (total length: 600 cm, 50 cm extending into the chamber, ID: 5.33 mm). During the β-pinene ozonolysis and limonene ozonolysis/NO_3 oxidation experiments, the inlet flow was kept at 0.6 l min^{-1} resulting in a sample residence time of 13.4 s. During the β-pinene/limonene mixture ozonolysis and the real tree emissions ozonolysis experiments, the inlet flow was increased to 1.6 l min^{-1} resulting in a sample residence time of 5.0 s.

2.3.3 TD – PTR-ToF-MS

The Thermal-Desorption unit was coupled to a commercial PTR-TOF8000 instrument (Ionicon Analytik GmbH, Austria). The TD is a dual aerosol inlet system consisting of impact collection thermal desorption cells. The setup was already used in several campaigns as described by Holzinger et al. (2013); (2010a).

In short, the centrepiece of both aerosol inlets is a Collection Thermal Desorption cell (CTD, Aerosol Dynamics, Berkeley, CA, USA), on which humidified ambient particles in the size range of 70 nm to 2 μm at an air sample flow rate of ~6 L min^{-1} are collected by impaction onto a stainless steel collection surface using a sonic jet impactor. The humidification of the aerosol sample flow to approximately 70% is achieved by a Nafion based humidifier and reduces particle rebound. All tubing in contact with volatilized aerosol compounds (i.e. the CTD cell, and all transfer tubing and valves) is coated to increase the chemical inertness of the surface. The CTD cell coating is AMCX (AMCX, L.L.C., Lemont PA, USA); all other parts received the Siltek®/Sulfinert®- treatment. The transfer lines are operated at elevated temperatures of 200 ℃ to avoid re-condensation of desorbed aerosol compounds.

In this study, aerosols were sampled from the chamber through a ~5 m long copper line (ID=6.5 mm). The operation of the system was fully automated. One cycle was completed in 2.5 h and included the analysis of (i) the first aerosol inlet (namely inlet A), (ii) the second aerosol inlet (namely inlet B), (iii) inlet A and (iv) inlet B that sampled particle-filtered chamber air, and (v) the analysis of gas-phase in conventional PTR-MS mode. The duration of each section was 30 min. Due to lab air contamination the conventional PTR-MS gas-phase measurements of the chamber air were not available from the TD-PTR. In addition, inlet A data quality was affected by a systematic change of the PTR-MS conditions (E/N fluctuation during background measurements caused by a malfunctioning valve). Consequently, inlet A data were excluded from this campaign.

The aerosols were pre-concentrated onto the CTD cell for 30 min with a flow of 6 L min^{-1} before thermal desorption into the PTR-MS. After collection, a small flow of ~ 10 mL min^{-1} of nitrogen carrier gas transported all compounds desorbing from the CTD cell directly into the PTR-MS. Aerosol compounds were thermally released from the CTD-cell by ramping the temperature up to 350 ℃ from room temperature (normally, 25 ℃). Temperature ramped continuously at a rate of ~15 ℃ min^{-1} for ~21 minutes until 350 ℃ followed by a dwell time of 3 minutes (at 350 ℃). After a cool down period of 6 min a new collection was initiated. For the last experiment (tree emissions), a denuder was installed on inlet B to constrain a possible artefact from gas-phase compounds adsorbing on the CTD cell.

The aerosol background was measured every other run by passing the airstream through a Teflon membrane filter (Zefluor 2.0 μm, Pall Corp.) that removed the particles from the air stream (sections: iii and iv mentioned above). The effective removal of particles was confirmed by test measurements with a condensation particle counter (TSI, WCPC Model 3785). While particles are removed by the Teflon filter, gas-phase compounds should be less affected. Filter samples to determine the aerosol background have been taken by turns: in each cycle, inlet A and inlet B sampled successively for 30 min of each, then the samples collected through the two inlets were analysed successively as well.

The PTRMS measures mixing ratios of compounds desorbed from aerosols in a nitrogen carrier gas. The mass concentration of an aerosol compound in the air sample is calculated according to

$$\mathbf{n_{aer,x}} = \mathbf{C_{mean,x}} \times \frac{\mathbf{F_{N_2}} \times \mathbf{t_{meas}}}{\mathbf{22.4} \times \mathbf{F_{col}} \times \mathbf{t_{col}}}, \qquad \textbf{(2)}$$

where $n_{aer,x}$ is the aerosol concentration of compound X in μg m^{-3}, $C_{mean,x}$ its (arithmetic) mean mixing ratio during the aerosol analysis in the nitrogen carrier gas in nmol mol^{-1}, MW_x the molecular weight of compound X in g mol^{-1}, F_{N2} the flow of the carrier gas in standard liters per minute, t_{meas} the duration of the aerosol measurement in minutes, F_{col} the flow rate at which the aerosols are collected in standard liters per minute, t_{col} the duration of aerosol collection in minutes and 22.4 the volume one mole of an ideal gas will occupy in liters. Mixing ratios of most compounds were calculated according to the method described in Holzinger et al. (2010b), which involves the use of default reaction rate constants (3×10^{-9} cm^3 s^{-1} $molecule^{-1}$),

Specific conditions during the campaign were as follows: E/N = 1.6×10^{-19} V m^2 $molec^{-1}$ (i.e. 160 Townsend units) to ensure ionization only by H_3O^+, temperature of the drift tube Td = 120 ℃, and a mass resolution of m/Δm ≈ 4000.

Mass spectra were obtained on a 5s time resolution. The data were processed using the PTRwid software (Holzinger, 2015). The software has several unique features including autonomous and accurate calibration of mass scale and the export of a uniform peak list which avoids the same ion being attributed to a slight different mass within the limits of precision. In total, 543 organic ions represented in the "unified mass list" have been obtained.

3 Results and discussions

In order to compare the different measurement techniques a time synchronization of the three data sets was performed. All data presented in this work have been synchronized to the ACM time with a time resolution of 4 hours. The presented time is the center of the sampling interval for all experiments.

3.1 Comparison of PTR-based aerosol measurement techniques to SMPS and AMS

Comparison of the different aerosol chemical characterization techniques to the AMS and SMPS was performed by means of linear regression (Figure 1). Since no collection efficiency (CE) was applied to the PTR-based aerosol measurement techniques, AMS data were treated the same way throughout this work, thus no AMS CE was enforced. SMPS organic mass concentration was calculated assuming a density of 1.4 g cm^{-3}, a valid assumption for SOA (Cross et al., 2007), that represented more than 98 % of the mass as observed from AMS. Each aerosol technique was collecting/detecting particles in different size ranges (Table 2). The volume distribution derived from

SMPS measurements (Figure S3) covered a particle diameter range of 100 to 400 nm which is within the size detection limits of all applied aerosol techniques.

A least orthogonal distance regression linear fit function, included in the IGOR extension ODRPack95, was used for each instrument related to SMPS data. Results suggested that the measured fraction compared to the SMPS mass was constant for each technique throughout the campaign. Due to experimental flaws $CHARON_{100}$ introduced a higher than usual variability of the particle enrichment in the aerodynamic lens during two experiments, the β-pinene ozonlysis and limonene ozonolysis/NO_3 oxidation (Section 2.3.2). These experiments were excluded when applying the linear fit. $CHARON_{100}$ was able to measure 80% ($1\sigma = \pm$ 10%) of the SMPS mass. ACM and AMS measured 51% (± 5%) and 67% (± 10%) while TD measured 27% (± 3%) of the SMPS, respectively. TD and ACM showed the lowest slope variability (≤ 5%), thus the highest stability in terms of recovery or overall detection efficiency. $CHARON_{100}$ and AMS followed with accuracy of ~ 10%, but at higher recovery rates. All instruments showed linear fit offset values close to zero when taking into account the error of the fit ($\pm 3\sigma$).

For the PTR based techniques and AMS a mass recovery underestimation could be expected due to a variety of processes from (i) the unideal CE during particle enrichment, (ii) thermal dissociation during desorption, (iii) incomplete evaporation or transmission, (iv) ionic dissociation in the ionization region and (v) the inability to ionize the reactant/fragment. The extent to which these processes affect the different techniques was investigated in detail and presented in the following by tracking the path of the particles from collection to detection.

It is well known that AMS derived mass concentrations have to be corrected for CE due to particle bounce signal loss on the vaporizer (Canagaratna et al., 2007). Fresh biogenic SOA though have a high CE (Kiendler-Scharr et al., 2009) and reduced bouncing effect, also observed from the relatively high AMS CE in this work (~ 0.7). ACM and TD utilize a collection surface as well and therefore introduce a CE uncertainty with the TD setup reducing even further the bouncing effects by humidifying the particles prior to collection. CHARON is an on-line technique avoiding the latter loss processes thus increasing the ability of the instrument to measure the mass concentration of the compounds generated during these experiments.

During desorption, thermal dissociation of molecules could introduce two or more fragmentation products. Canagaratna et al. (2015) reported that in the AMS organics gave rise to H_2O^+, CO^+ and CO_2^+ signal due to surface evaporation and thermal break down of organic molecules at vaporizer operating temperatures down to 200 °C (under vacuum conditions). Although neutral dissociation products like H_2O, CO and CO_2 could be ionized by the AMS, their proton affinities are lower than that of H_2O, thus PTR techniques would no longer ionize and detect them. On the contrary, remaining smaller organic fragmentation products with proton affinities higher than H_2O would still be visible to the PTR-MS. A lack of detection of certain neutral fragments formed during thermal desorption could introduce an underestimation of the total mass, oxygen and carbon concentration for the PTR based techniques. It should be noted that decarboxylation and dehydration reactions are strongly dependent on the temperature, pressure and the heat exposure time of the molecules. CHARON was operated at the lowest temperature of 140 °C, under a few mbars of pressure and with the lowest heat exposure time thus avoiding the latter reactions. On the contrary, ACM and TD were operated at 1 bar and up to 250 °C and 350 °C respectively with longer heat exposure times. To further assess whether surface evaporation for ACM and TD had an additional effect

on the measurements, focus was given on the experimental case studies performed by Salvador et al. (2016) using the TD-PTR-ToF-MS. Five authentic standard substances (phthalic acid, levoglucosan, arabitol, *cis*-pinonic and glutaric acid) were utilized to examine the response of the sampling device. If the compounds would only fragment in the PTR-ToF-MS due to ionic dissociation, then the detected fragments should have the same volatility trend as the parent compounds since both originate from the latter. During desorption of the collected samples, fragment ions were found to represent different volatility trends compared to their parent ions (Arabitol, cis-Pinonic Acid). These thermogram differences, originating from the same substance, promoted a certain amount of neutral fragmentation/pyrolysis in the hot TD cell.

The thermal desorption process varied for the different PTR-based inlet techniques with different desorption residence times, desorption temperatures and pressure conditions (see section 2.3). Although CHARON was operated at lower temperatures compared to ACM and TD, its reduced pressure compensated for the temperature difference thus increasing the volatility range down to LVOC (Eichler et al., 2017). It could still be though that a fraction of the SOA mass in the extremely low volatility OC (ELVOC) range will not evaporate during desorption from any of the systems studied. If this effect would be significant it would be more pronounced in the presence of high percentages of ELVOCs in the aerosol, i.e. during periods with increased O:C ratios (indicated in Figure 2). A non-linear relationship between SMPS and the PTR based techniques would be the result, which has not been observed (Figure 1). We therefore concluded that incomplete evaporation of ELVOC constitutes a minor contribution to the mass recovery underestimation. Transmission losses of OA vapours on the pathway from evaporation to detection could occur on cold spots in between the evaporation zone and the drift tube. All components were heated to higher temperatures than the evaporation zone in order to avoid these losses. Within the drift tube of the PTR the temperature is lower than in the evaporation zone but the lower pressure will reduce but not exclude the possibility of re-condensation of organic vapours.

Ionic dissociation in the ionization region of the PTR-MS is strongly affected by the PTR operating conditions and in particular the E/N applied (Section 2.3). The lower mass concentration detected by the TD unit compared to the other techniques could be partly explained by the different E/N used, with TD operated at the highest E/N = 160 Td. This high potential of fragmentation losses during quantification would be given as:

$$(R^+)^* \rightarrow F^+ + N \quad (3)$$

where $(R^+)^*$ is the unstable protonated reactant, F^+ is the protonated fragment and N is the neutral product. Commonly occurring neutral fragments are H_2O from organic hydroxyl functional groups or HNO_3 from organic nitrate functional groups. While the former is often observed, during our studies organic nitrate fragmentation has not been observed as their formation is hindered during our experiments due to low NOx-conditions. This has been supported by AMS derived organic nitrate measurements being below 10% (Figure S4). By increasing the fragmentation potential the neutral products would increase thus lowering the total mass concentration detected. This could also lead to an underestimation of the ACM mass concentration compared to $CHARON_{100}$ (ACM operated at 120 Td and $CHARON_{100}$ at 100 Td) and is discussed in detail in Section 3.2. It should be noted that the mass underestimation of the ACM due to ionic and thermal dissociation could be higher than 16% (the mass difference between the ACM and AMS). This would imply that ACM CE was higher compared to the AMS CE

during this campaign, a possible result in view of the differences of vaporizer/collector geometry (Hohaus et al., 2010).

Additional comparison between the AMS and the PTR-ToF-MS based techniques was examined by determining the bulk oxygen to carbon ratio (O:C) for all instruments (Figure 2). AMS O:C values were calculated based on the method by Canagaratna et al. (2015). All instruments followed similar trends. O:C ratios increased with photochemistry initiation (chamber illumination) or NO_3 oxidation (limonene experiment/NO injection). On the contrary, O:C values decreased when fresh BVOC was introduced into SAPHIR and additional SOA was formed during the tree BVOCs re-emission stage (11 – 22 h after ozone injection). When compared to AMS, all PTR-ToF-MS based techniques showed lower O:C values. Good agreement was found between the ACM and TD O:C values (< 3% difference). $CHARON_{100}$ measured higher O:C compared to ACM and TD (ACM lower by ~ 20-35%), an indication that during this campaign $CHARON_{100}$ was capable of detecting more oxygenated compounds. When comparing the β-pinene and limonene experiments, $CHARON_{100}$ had increased O:C values for experiments that incorporated β-pinene while ACM had the opposite behavior, with higher O:C during the limonene experiment. For the tree emissions experiment the BVOC system resulted in SOA that showed increased O:C values for all instruments introducing compounds with higher oxygen content in the particulate-phase. During this experiment CHARON was operated at different E/N operating conditions thus providing further insights of the influence of E/N on O:C values (Figure S5). Results showed that O:C increased by approximately 10% when changing the CHARON E/N from 100 Td to 65 Td, thus providing softer ionization conditions.

Although nearly all $C_xH_yO_z$ ions can be identified and quantified within the AMS mass spectra, AMS O:C calculation based on Canagaratna et al. (2015) has several sources of uncertainties due to correction factors applied. As stated by Canagaratna et al. (2015), the overall errors observed in elemental ratios calculations would introduce an upper uncertainty of 28%. In contrast to AMS data O:C ratios for the PTR based techniques were calculated with no additional correction factors thus explaining their lower values when compared to AMS.

PTR-ToF-MS is considered a soft ionization technique which suffers less from fragmentation and therefore should provide O:C ratios closer to the true values compared to uncorrected AMS data. Nevertheless, water clustering and fragmentation could occur, either increasing or decreasing O:C ratios. When proton transfer reactions induce fragmentation a neutral fragment is lost. For oxygenated organics it has been shown that the loss of water as neutral fragment is a common fragmentation pathway (de Gouw and Warneke, 2007). This could explain the lower O:C values seen from CHARON, ACM and TD compared to the AMS. Intercomparison of the PTR based techniques further showed that $CHARON_{100}$ was more sensitive to oxygenated compounds compared to ACM and TD. Higher O:C ratios were observed when comparing $CHARON_{65}$ to $CHARON_{100}$ indicating that low E/N values can decrease the loss of neutral fragments such as water or carbon containing compounds with O:C ratios >1 (e.g. CO_2, HCOOH). This factor does affect the ACM and TD O:C ratios even more, since they are operated at even higher E/N (120 Td and TD at 160 Td, respectively) than CHARON. It should be noted that lower E/N values could also increase the tendency to detect water clusters, i.e. $AH^+(H_2O)_n$, where A is the ionized organic compound, bearing the risk to bias the O:C ratio high which is explored further in the next section.

As previously discussed, AMS H_2O^+, CO^+ and CO_2^+ signals are generated due to surface evaporation at temperatures exceeding 200 °C (under vacuum conditions). These fragment signals cannot be detected from ACM and TD (that also undergo surface evaporation compared to CHARON), thus an additional underestimation of their O:C values could not be excluded. To assess the extent of surface fragmentation, further re-calculation of the AMS O:C, excluding the H_2O^+, CO^+ and CO_2^+ peaks (Figure S6) was performed and compared to the PTR-based techniques. Results showed that AMS O:C ratios were lower than O:C ratios of ACM and TD. When only excluding the H_2O^+ signal, AMS O:C ratios were higher than those of ACM and TD. These results suggest that CO and CO_2 loss by thermal dissociation in the ACM and TD play a less significant role compared to AMS due to their lower operating evaporation temperatures and higher pressure.

When comparing experiments incorporating β-pinene or limonene, the different behavior of the O:C ratios found for the $CHARON_{100}$ ($O{:}C_{\text{ CHARON, limonene}} < O{:}C_{\text{ CHARON, β-pinene}}$) and ACM ($O{:}C_{\text{ ACM, limonene}} > O{:}C_{\text{ ACM, β-pinene}}$) could be due to different fragmentation patterns of the particulate-phase functional groups or due to their volatility differences. Since limonene SOA are less volatile than β-pinene SOA (Lee et al., 2011) a fraction of the OA oxygenated mass that would evaporate at higher temperatures could be lost, thus leading to lower O:C values compared to the β-pinene experiments. However, ACM showed only minor volatility differences when comparing the β-pinene to the limonene experiments, as seen in Figure S7. Although CHARON was operated at lower temperatures compared to ACM, its reduced pressure compensated for the temperature difference thus increasing the volatility range down to LVOC (Eichler et al., 2017). These results conclude that differences in the O:C trends of ACM and CHARON could not be explained by changes of the SOA volatility. The ionic and thermal dissociation patterns of the different particulate-phase functional groups could play a role in these findings and has to be examined in future studies.

3.2 Classification of SOA composition

Further comparison of the aerosol chemical characterization techniques was performed with a focus on the different chemical characteristics (oxygen content, carbon content, molecular weight) of the SOA composition. A desorption period from the tree emissions experiment, 25 hours after the ozone injection (Figure 2 (d)), was chosen in order to highlight the instrument performance differences, shown in Figure 3. The mass concentration of all compounds containing the same carbon number was calculated. These carbon fractions were then further separated depending on the number of oxygen atoms the compounds contained. The molecular weights (MW) of the SOA constituents was separated in five different *m/z* range groups, from *m/z* 30 - 50, *m/z* 50 - 100, *m/z* 100 - 150, *m/z* 150 - 250, *m/z* >250. All instruments showed similar carbon content distributions, with the highest concentration introduced from C8 compounds. CHARON was able to measure compounds in the C10 - C20 range while ACM and TD only detected up to C13 compounds. The overall OA mass concentration decreased when moving from lower ($CHARON_{65}$ and $CHARON_{100}$) to higher E/N values (ACM at 120 Td and TD at 160 Td). The same trend was seen for the oxygen content of compounds; with a characteristic example being the compounds containing 5 oxygen atoms that decreased by a factor of 2 with the same instrument but different operational parameters for the PTR-ToF-MS ($CHARON_{65}$ vs. $CHARON_{100}$). In ACM and TD compounds containing 5 oxygens were negligible. A

506 similar trend was observed for *m/z* range distributions, with a higher fraction of low *m/z* compounds observed at increasing E/N values. ACM and TD results indicated that the main fraction of compounds was detected for MW <
508 100 amu (70 and 75% of the overall mass concentration, respectively).

These results clearly show the high dependency of the overall mass concentration detection as well as the carbon,
510 oxygen and MW content determination being strongly affected by the PTR-ToF-MS E/N operating conditions. As the E/N values increased, fragmentation increased leading to undetected neutral fragments. This loss of information
512 directly affects the overall mass concentration and MW detection range. Comparing the ACM to the TD MW pie charts showed that, although ACM was operated at lower E/N conditions (120 Td) than the TD (160 Td) the
514 contribution in the lower MW range was higher for the ACM. The reason for this dissimilarity could be due to the lower resolution and the higher limit of detection of the PTR-ToF-MS used for the ACM (see Table 2) leading to
516 lower detection of the higher molecular weight compounds. Since water loss is the major fragmentation occurring in the PTR-ToF-MS, the oxygen content is affected the strongest. This could explain why compounds with 5 oxygens
518 were nearly undetectable for ACM and TD compared to CHARON.

To further assess the differences in chemical classification by each instrument the relative OA mass concentration of
520 molecular carbon, oxygen and weight (box-and-whiskers including all data points throughout the campaign) were used, as seen in Figure 4. ACM and TD showed similar distributions for all contributions throughout the campaign
522 with only minor differences (< 3%). On the contrary, their comparison to $CHARON_{100}$ showed a clear difference. Compounds in the lower MW range (< *m/z* 150), containing lower molecular carbon (< 9 carbon atoms) and oxygen
524 (< 2 oxygen atoms) showed higher contributions for the ACM and TD compared to $CHARON_{100}$. A detailed comparison of CHARON's different E/N conditions during the tree emissions experiment (Figure S8) was also
526 performed. Results indicated that for lower E/N, an absolute difference of 2%, 5% and 10% for the molecular carbon, weight and oxygen contributions were observed, respectively, suggesting that in this E/N range (from 65 to
528 100 Td) fragmentation is dominated by oxygen containing functional groups loss.

The above results strongly suggest that the E/N settings play a key role to the fragmentation patterns. By increasing
530 the drift tube voltage, the velocity of the ions increased, leading to higher kinetic energy in ion molecule and therefore stronger buffer gas collision. This energy increase was translated to an increase in fragmentation. On the
532 contrary, the lower the E/N was set, the higher the sensitivity due to enhanced reaction times but also the stronger the cluster ion distribution change, supporting more $H_3O^+(H_2O)_n$ (n=1,2,3) cluster ion generation (de Gouw and
534 Warneke, 2007). In order to quantify whether the PTR-ToF-MS E/N conditions were a major factor for the differences seen during this campaign, a case study of pinonic acid was performed in the lab. Monodisperse pinonic
536 acid particles were generated (900 – 1100 particles/cm^3) and directed to a CHARON-PTR-ToF-MS, changing E/N values from 60 to 170 Td (Figure S9). Results showed that the relative intensity of the parent ion decreased rapidly
538 when increasing the E/N values. At the same time, the relative intensity of the lightweight fragments was increasing. The effect of the parent ion clustering with water was negligible suggesting no overestimation of the CHARON
540 oxygen content at low E/N (65 Td). By assuming a uniform sensitivity and calculating the total signal (parent ion and fragments, assuming all *m/z* represent parent molecules) the mass fraction of pinonic acid particles was
542 calculated (Figure S10). The higher the E/N values were set, the less the PTR-ToF-MS measured compared to the

SMPS. These results confirmed our previous findings that fragmentation losses lead to an underestimation of the overall mass concentration. Therefore the different E/N conditions of the detection systems (PTR-ToF-MS) could explain in a large fraction the differences between the CHARON, ACM and TD oxygen and carbon content (results seen in Figure 2 and Figure 4) as well as their differences in the overall detectable mass (results seen in Figure 1 and Figure 3). A clear influence of the aerosol sampling technique on the differences of these parameters cannot be determined nor excluded (Salvador et al., 2016).

3.3 Volatility comparison

During the campaign, CHARON was operated at a constant temperature (140 °C) while ACM and TD ramped through different temperatures during desorption of the collected aerosol samples (see Section 2). The ramping of ACM and TD provided the possibility of a detailed comparison of the compound dependent volatility trends. In Figure 5 the timeseries of ACM and TD for the β-pinene, the β-pinene/limonene mixture and the tree emissions experiments were investigated. The limonene ozonolysis and NO_3 oxidation was excluded from this comparison, due to TD operational problems. For both instruments high contributions of the aerosol mass concentration evaporated at lower temperatures when fresh SOA were generated (initial hours of the experiments and tree emissions A_o stage), hence higher SOA volatility values were observed. As oxidation continued the relative contributions of aerosol mass evaporating at low temperatures and therefore the overall volatility decreased. When illuminating the chamber, SOA volatility decreased suggesting that photochemical aging of the SOA took place leading to a change of the chemical composition and volatility distribution. For experiments having β-pinene as a precursor for the subsequent SOA formation, TD showed a decreasing volatility as the experiment evolved while ACM reached a plateau after 5 to 10 hours of aging.

The volatility changes for both instruments, during the initial hours of the experiments and during the re-introduction of BVOCs for the trees experiment, could be attributed to the high concentration semi-volatile organic compounds (SVOCs) in the gas-phase that had the maximum available surface to condense on (SMPS at its maximum surface area and mass concentration). Under these conditions, these compounds would partition more to the particulate-phase thus increasing their contribution during the highest concentration periods. These easier to evaporate SVOCs could change the volatility patterns by a change of the thermograms during the maximum concentration periods, as observed from both techniques. Discrepancies between the ACM and TD, with the latter having a steadily changing desorption temperature with time, could be affected by several operating differences. During evaporation ACM was ramped by 100 °C min^{-1} to a maximum of 250 °C, with 3-minute isothermal sections at 100 °C, 150 °C and 250 °C, respectively, while TD was ramped continuously at a rate of ~15 °C min^{-1} for ~21 minutes until 350 °C. The higher volatility resolution of TD compared to ACM could introduce an increased sensitivity to volatility changes thus increase the TD variability compared to ACM. Differences could be partly attributed to the different design of the instruments. ACM ensured complete separation of the particulate from the gas-phase (> 99.9999 gas-phase removal) while TD was corrected for gas-phase contamination by performing background measurements (Section 2). As the collection of the particulate-phase compounds was performed for the TD, the collector was exposed to high concentration of SVOCs from the gas-phase, thus increasing the absorption of

these compounds to the particulate-phase. As the gas-phase concentrations decreased the TD volatility decreased. This could thus indicate a possible background correction artifact mostly affecting compounds in the higher volatility range, evaporating in the first temperature steps (100 ºC). It should be noted that after the β-pinene initial hours of consumption, secondary reactions in the absence of light and the presence of ozone should be negligible due to the lack of unsaturated reactants. The expected temporal volatility behavior would thus be shifted towards a more stable instead of changing volatility system.

To further assess the volatility differences of ACM and TD, focus was given on the molecular oxygen number based on the assumption that oxygen number correlates to volatility (Jimenez et al., 2009). Box-and-whiskers, including all campaign desorption periods, were generated for each molecular oxygen number at each temperature, as seen in Figure 6. The data were normalized to the sum of the measured mass concentration from each molecular oxygen number in all temperatures (top equation in Figure 6). Results showed that TD had a broader range in fractional contribution for all oxygen bins when compared to the ACM. A characteristic temperature showing this difference was at 150 °C, where TD showed results in the range of 0.2 to 0.55 while ACM was in the range from 0.15 to 0.25. Despite the differences in relative contribution, both instruments showed similar trends. As the collector temperature increased oxygenated compounds (2, 3 and 4 oxygens) contributed more than lower oxygenates. On the contrary, at lower temperatures compounds containing 0 and 1 oxygen were the dominant factor. Overall, for ACM around 20% of the SOA evaporated at 100 °C, 20% at 150 °C and 60% at 250 °C. TD showed similar volatility trends with 15 to 20% of the SOA evaporating at 100 °C, 35% at 150 °C and 50 to 55% at 250 °C.

According to observations and theory (Jimenez et al., 2009) oxygenated compounds are expected to have lower volatility thus evaporating at higher temperatures. TD and ACM described the expected volatility trends during the performed experiments based on compound specific information in accordance to theory. The variability of TD compared to ACM reflected the differences in the design and operation of the individual systems described previously. The higher volatility resolution but also the higher E/N conditions of TD could explain most of the observed discrepancies. Fragmentation due to ionic dissociation after the evaporation could influence the volatility molecular oxygen content distribution by loss of neutral oxygen containing fragments. This could further affect the volatility distribution when the oxidation product concentrations change with time, reflected by the increase of the O:C ratios (see Figure 2). Furthermore, the ability of ACM to achieve complete gas to particle separation resulted in a lower thermogram uncertainty in the higher volatility range thus smaller variations. These results show the applicability of both techniques to study BSOA volatility trends in a compound specific level.

3.4 Compound detection comparison and tracers attribution

The molecular formula ($C_xH_yO_zN_a$) was attributed to each detected signal derived from the exact molecular mass (see Section 2) determined by the TOF-MS for all 3 techniques throughout the campaign. In order to assess whether major contributing molecules with the same chemical characteristics were determined by all instruments, a comparison of the dominant signals was performed i.e. the molecular formulas that (i) were measured by all techniques during each experiment and (ii) were within the 80 highest signal concentrations. Figure 7 shows the respective results from the BSOA detected in the C7 to C10 range with varying oxygen content (from 0 to 4

oxygens). Although these techniques could provide the molecular formula of the compounds, the molecular structures are unknown. In order to derive further information, comparison to previous publications was performed for the major oxidation products from (a) the β-pinene ozonolysis (Chen and Griffin, 2005; Hohaus et al., 2015; Jenkin, 2004; Yu et al., 1999), (b) limonene ozonolysis and NO_3 oxidation (Chen and Griffin, 2005; Jaoui et al., 2006; Kundu et al., 2012; Leungsakul et al., 2005a; Leungsakul et al., 2005b) and (c) tree emissions ozonolysis with α-pinene and Δ^3-carene being the major reactants (Chen and Griffin, 2005; Praplan et al., 2014; Yu et al., 1999). Results showed that all techniques were able to detect most of the expected molecules. Details on the molecular formula and suggested structure are provided in more detail in Table S1. Due to fragmentation most of the compounds were not detected at the parent ion molecular weight but underwent water loss in accordance to the findings that O:C ratios are observed to be reduced by ACM, TD and CHARON compared to the AMS (see Section 3.1). These compounds corresponded to a large fraction of the BSOA mass measured from each technique (bars in Figure 7). On average,70%, 60%, and 40% of the measured mass was contributed from these compounds, for ACM, CHARON and TD respectively. When comparing the above compounds concentration to the SMPS total mass, around 30%, 50% and 10% of the SMPS mass for ACM, CHARON and TD respectively was explained. The overlapping of detected compounds to previous publications (theoretical and experimental work) and their high contribution (up to 50%) to the overall BSOA mass concentration strongly promotes the use of PTR-ToF-MS aerosol measurement techniques to gain valuable insight on the chemical characteristics of BSOA.

4 Conclusions

A comparison of three different aerosol chemical characterization techniques has been performed as part of a chamber study on fresh and photochemically aged BSOA, formed from the ozonolysis of monoterpenes. The aerosol collection module (ACM), the chemical analysis of aerosol on-line (CHARON) and the collection thermal desorption unit (TD) are different aerosol sampling inlets utilizing a PTR-ToF-MS. These techniques were deployed in a set of chamber experiments at the atmosphere simulation chamber SAPHIR to investigate SOA formation and aging from different monoterpenes (*β*-pinene, limonene) and from real plant emissions (Pinus sylvestris *L.*).

The total aerosol concentration recovery of the PTR based techniques, compared to an SMPS, was 80 ± 10%, 51 ± 5% and 27 ± 3% for CHARON, ACM and TD respectively. In contrast, an AMS concurrently operated and with no collection efficiency correction applied, showed a recovery of 67%. The three PTR based techniques were capable of measuring the same major contributing signals for the different monoterpene oxidation products studied. These attributed compounds corresponded to a high fraction of the overall SOA mass concentration with 30%, 50% and 10% of the overall mass being explained for ACM, CHARON and TD respectively. Additional comparison to previous publications showed that these compounds corresponded to known products of the monoterpenes studied. Both the ACM and TD collection and thermal desorption design provided additional information on their volatility and showed similar trends. Compounds containing higher molecular oxygen number (≥ 2) contributed more to the aerosol fraction desorbed at high temperatures than lower oxygenated compounds (molecular oxygen number < 2) which were more efficiently desorbed at low temperatures.

Oxygen to carbon ratios (O:C) increased while SOA production and aging proceeded. All instruments had comparable O:C trends during the course of an experiment. Good agreement was found for the ACM and TD O:C values (< 3% difference) while CHARON showed 20 to 35% higher O:C ratios.

Despite significant difference in the aerosol collection and desorption techniques, the major reason for the discrepancies was the different operating conditions of the PTR-ToF-MS. Laboratory case studies supported that E/N conditions played a crucial role in fragmentation leading to lower O:C ratios at high E/N. Since ACM and TD were operated at higher E/N compared to CHARON this resulted to higher fragmentation, thus affecting their oxygen and carbon content and mass recovery. Compared to AMS, PTRMS is a soft ionization technique even at high E/N and therefore less prone to fragmentation. AMS requires correction factors (Canagaratna et al., 2015), to determine O:C ratios wereas for PTRMS corrections were omitted. Determination of O:C ratios for the PTR based techniques was thus underestimated, explaining their difference to the HR-ToF-AMS (30 to 50% higher). Differences in the sampling and evaporation technique might introduce also deviations between the chemical characterizations i.e. due to thermal decomposition. This has to be studied in detail in future comparisons by operating the PTR-ToF-MS instruments under the same E/N conditions.

The ability of all PTR based techniques to measure compounds, supported from previous publications, strongly promotes their use. These techniques can provide valuable insight on the chemical characteristics of freshly formed and aged BSOA, and on thermodynamic properties such as partitioning coefficient values and volatility patterns on a compound specific level.

Author contribution

RT , RH, AW and AKS designed the experiments. TH and RT operated the chambers. SHS, PS, PE, MM, KM, GIG, RW, MK, AW, RH and RT conducted the data collection and evaluation for AMS, TD, CHARON, ACM, PTR and GC-MS. MM designed and carried out the laboratory characterization experiments. GIG, RT, TH and AKS did the data analysis. GIG did the data interpretation and prepared the manuscript with contributions from all co-authors.

Acknowledgements

This work is supported by the EC's 7th Framework Program under Grant Agreement Number 287382 (Marie Curie Training Network PIMMS), by the Helmholtz President's Fund (Backfeed), and by the Dutch NOW Earth and Life Science (ALW), project 824.14.002.The authors acknowledge support by the SAPHIR teams, electronic and mechanical workshops.

References

Aiken, A. C., P. F. DeCarlo, J. H. Kroll, D. R. Worsnop, J. A. Huffman, K. S. Docherty, I. M. Ulbrich, C. Mohr, J. R. Kimmel, D. Sueper, et al.: O/C and OM/OC Ratios of Primary, Secondary, and Ambient Organic Aerosols with High-Resolution Time-of-Flight Aerosol Mass Spectrometry, *Environ Sci Technol*, *42*(12), 4478-4485, doi:10.1021/es703009q, 2008.

Canagaratna, M. R., J. T. Jayne, J. L. Jimenez, J. D. Allan, M. R. Alfarra, Q. Zhang, T. B. Onasch, F. Drewnick, H. Coe, A. Middlebrook, et al.: Chemical and microphysical characterization of ambient aerosols with the aerodyne aerosol mass spectrometer, *Mass Spectrom Rev*, *26*(2), 185-222, doi:10.1002/mas.20115, 2007.

Canagaratna, M. R., J. L. Jimenez, J. H. Kroll, Q. Chen, S. H. Kessler, P. Massoli, L. Hildebrandt Ruiz, E. Fortner, L. R. Williams, K. R. Wilson, et al.: Elemental ratio measurements of organic compounds using aerosol mass spectrometry: characterization, improved calibration, and implications, *Atmospheric Chemistry and Physics*, *15*(1), 253-272, doi:10.5194/acp-15-253-2015, 2015.

Chen, J., and R. Griffin: Modeling secondary organic aerosol formation from oxidation of -pinene, -pinene, and -limonene, *Atmospheric Environment*, *39*(40), 7731-7744, doi:10.1016/j.atmosenv.2005.05.049, 2005.

Cross, E. S., J. G. Slowik, P. Davidovits, J. D. Allan, D. R. Worsnop, J. T. Jayne, D. K. Lewis, M. Canagaratna, and T. B. Onasch: Laboratory and Ambient Particle Density Determinations using Light Scattering in Conjunction with Aerosol Mass Spectrometry, *Aerosol Science and Technology*, *41*(4), 343-359, doi:10.1080/02786820701199736, 2007.

de Gouw, J., and C. Warneke: Measurements of volatile organic compounds in the earth's atmosphere using proton-transfer-reaction mass spectrometry, *Mass Spectrom Rev*, *26*(2), 223-257, doi:10.1002/mas.20119, 2007.

DeCarlo, P. F., J. R. Kimmel, A. Trimborn, M. J. Northway, J. T. Jayne, A. C. Aiken, M. Gonin, K. Fuhrer, T. Horvath, K. S. Docherty, et al.: Field-Deployable, High-Resolution, Time-of-Flight Aerosol Mass Spectrometer, *Analytical Chemistry*, *78*(24), 8281-8289, doi:10.1021/ac061249n, 2006.

Eichler, P., M. Müller, B. D'Anna, and A. Wisthaler: A novel inlet system for online chemical analysis of semi-volatile submicron particulate matter, *Atmospheric Measurement Techniques*, *8*(3), 1353-1360, doi:10.5194/amt-8-1353-2015, 2015.

Eichler, P., M. Müller, C. Rohmann, B. Stengel, J. Orasche, R. Zimmermann, and A. Wisthaler: Lubricating Oil as a Major Constituent of Ship Exhaust Particles, *Environmental Science & Technology Letters*, *4*(2), 54-58, doi:10.1021/acs.estlett.6b00488, 2017.

Goldstein, A. H., and I. E. Galbally: Known and Unexplored Organic Constituents in the Earth's Atmosphere, *Environ Sci Technol*, *41*(5), 1514-1521, doi:10.1021/es072476p, 2007.

Guenther, A. B., X. Jiang, C. L. Heald, T. Sakulyanontvittaya, T. Duhl, L. K. Emmons, and X. Wang: The Model of Emissions of Gases and Aerosols from Nature version 2.1 (MEGAN2.1): an extended and updated framework for modeling biogenic emissions, *Geoscientific Model Development*, *5*(6), 1471-1492, doi:10.5194/gmd-5-1471-2012, 2012.

Hallquist, M., J. C. Wenger, U. Baltensperger, Y. Rudich, D. Simpson, M. Claeys, J. Dommen, N. M. Donahue, C. George, A. H. Goldstein, et al.: The formation, properties and impact of secondary organic aerosol: current and emerging issues, *Atmos. Chem. Phys.*, *9*(14), 5155-5236, doi:10.5194/acp-9-5155-2009, 2009.

Hohaus, T., I. Gensch, J. R. Kimmel, D. R. Worsnop, and A. Kiendler-Scharr: Experimental determination of the partitioning coefficient of β-pinene oxidation products in SOAs, *Physical Chemistry Chemical Physics*, *17*(22), 14796-14804, doi:10.1039/C5CP01608H, 2015.

Hohaus, T., U. Kuhn, S. Andres, M. Kaminski, F. Rohrer, R. Tillmann, A. Wahner, R. Wegener, Z. Yu, and A. Kiendler-Scharr: A new plant chamber facility, PLUS, coupled to the atmosphere simulation chamber SAPHIR, *Atmospheric Measurement Techniques*, *9*(3), 1247-1259, doi:10.5194/amt-9-1247-2016, 2016.

Hohaus, T., D. Trimborn, A. Kiendler-Scharr, I. Gensch, W. Laumer, B. Kammer, S. Andres, H. Boudries, K. A. Smith, D. R. Worsnop, et al.: A new aerosol collector for quasi on-line analysis of particulate organic matter: the Aerosol Collection Module (ACM) and first applications with a GC/MS-FID, *Atmospheric Measurement Techniques*, *3*(5), 1423-1436, doi:DOI 10.5194/amt-3-1423-2010, 2010.

744 Holzinger, R.: PTRwid: A new widget tool for processing PTR-TOF-MS data, *Atmospheric Measurement Techniques*, *8*(9), 3903-3922, doi:10.5194/amt-8-3903-2015, 2015.
746
Holzinger, R., A. H. Goldstein, P. L. Hayes, J. L. Jimenez, and J. Timkovsky: Chemical evolution of organic aerosol
748 in Los Angeles during the CalNex 2010 study, *Atmospheric Chemistry and Physics*, *13*(19), 10125-10141, doi:10.5194/acp-13-10125-2013, 2013.
750
Holzinger, R., A. Kasper-Giebl, M. Staudinger, G. Schauer, and T. Röckmann: Analysis of the chemical
752 composition of organic aerosol at the Mt. Sonnblick observatory using a novel high mass resolution thermal-desorption proton-transfer-reaction mass-spectrometer (hr-TD-PTR-MS), *Atmospheric Chemistry and Physics*,
754 *10*(20), 10111-10128, doi:10.5194/acp-10-10111-2010, 2010a.

756 Holzinger, R., J. Williams, F. Herrmann, J. Lelieveld, N. M. Donahue, and T. Röckmann: Aerosol analysis using a Thermal-Desorption Proton-Transfer-Reaction Mass Spectrometer (TD-PTR-MS): a new approach to study
758 processing of organic aerosols, *Atmos. Chem. Phys.*, *10*(5), 2257-2267, doi:10.5194/acp-10-2257-2010, 2010b.

760 Isaacman, G., N. M. Kreisberg, L. D. Yee, D. R. Worton, A. W. H. Chan, J. A. Moss, S. V. Hering, and A. H. Goldstein: Online derivatization for hourly measurements of gas- and particle-phase semi-volatile oxygenated
762 organic compounds by thermal desorption aerosol gas chromatography (SV-TAG), *Atmospheric Measurement Techniques*, *7*(12), 4417-4429, doi:10.5194/amt-7-4417-2014, 2014.
764
Jaoui, M., E. Corse, T. E. Kleindienst, J. H. Offenberg, M. Lewandowski, and E. O. Edney: Analysis of Secondary
766 Organic Aerosol Compounds from the Photooxidation of d-Limonene in the Presence of NOX and their Detection in Ambient PM2.5, *Environ Sci Technol*, *40*(12), 3819-3828, doi:10.1021/es052566z, 2006.
768
Jenkin, M. E.: Modelling the formation and composition of secondary organic aerosol from α- and β-pinene
770 ozonolysis using MCM v3 *Atmos. Chem. Phys.*, *4*, 1741-1757, 2004.

772 Jimenez, J. L., M. R. Canagaratna, N. M. Donahue, A. S. H. Prevot, Q. Zhang, J. H. Kroll, P. F. DeCarlo, J. D. Allan, H. Coe, N. L. Ng, et al.: Evolution of Organic Aerosols in the Atmosphere, *Science*, *326*(1525),
774 doi:10.1126/science.1180353, 2009.

776 Jordan, A., S. Haidacher, G. Hanel, E. Hartungen, L. Märk, H. Seehauser, R. Schottkowsky, P. Sulzer, and T. D. Märk: A high resolution and high sensitivity proton-transfer-reaction time-of-flight mass spectrometer (PTR-TOF-
778 MS), *International Journal of Mass Spectrometry*, *286*(2–3), 122-128, doi:http://dx.doi.org/10.1016/j.ijms.2009.07.005, 2009.
780
Kanakidou, M., J. Seinfeld, S. Pandis, I. Barnes, F. Dentener, M. Facchini, R. V. Dingenen, B. Ervens, A. Nenes,
782 and C. Nielsen: Organic aerosol and global climate modelling: a review, *Atmospheric Chemistry and Physics*, *5*(4), 1053-1123, 2005.
784
Kiendler-Scharr, A., Q. Zhang, T. Hohaus, E. Kleist, A. Mensah, T. F. Mentel, C. Spindler, R. Uerlings, R.
786 Tillmann, and J. Wildt: Aerosol Mass Spectrometric Features of Biogenic SOA: Observations from a Plant Chamber and in Rural Atmospheric Environments, *Environ Sci Technol*, *43*(21), 8166-8172, doi:10.1021/es901420b, 2009.
788
Kreisberg, N. M., S. V. Hering, B. J. Williams, D. R. Worton, and A. H. Goldstein: Quantification of Hourly
790 Speciated Organic Compounds in Atmospheric Aerosols, Measured by an In-Situ Thermal Desorption Aerosol Gas Chromatograph (TAG), *Aerosol Science and Technology*, *43*(1), 38-52, doi:10.1080/02786820802459583, 2009.
792
Kundu, S., R. Fisseha, A. L. Putman, T. A. Rahn, and L. R. Mazzoleni: High molecular weight SOA formation
794 during limonene ozonolysis: insights from ultrahigh-resolution FT-ICR mass spectrometry characterization, *Atmospheric Chemistry and Physics*, *12*(12), 5523-5536, doi:10.5194/acp-12-5523-2012, 2012.
796

Lee, B.-H., J. R. Pierce, G. J. Engelhart, and S. N. Pandis: Volatility of secondary organic aerosol from the ozonolysis of monoterpenes, *Atmospheric Environment*, *45*(14), 2443-2452, doi:10.1016/j.atmosenv.2011.02.004, 2011.

Leungsakul, S., M. Jaoui, and R. M. Kamens: Kinetic Mechanism for Predicting Secondary Organic Aerosol Formation from the Reaction of d-Limonene with Ozone, *Environ Sci Technol*, *39*(24), 9583-9594, doi:10.1021/es0492687, 2005a.

Leungsakul, S., H. E. Jeffries, and R. M. Kamens: A kinetic mechanism for predicting secondary aerosol formation from the reactions of d-limonene in the presence of oxides of nitrogen and natural sunlight, *Atmospheric Environment*, *39*(37), 7063-7082, doi:10.1016/j.atmosenv.2005.08.024, 2005b.

Liu, P., P. J. Ziemann, D. B. Kittelson, and P. H. McMurry: Generating Particle Beams of Controlled Dimensions and Divergence: I. Theory of Particle Motion in Aerodynamic Lenses and Nozzle Expansions, *Aerosol Science and Technology*, *22*(3), 293-313, doi:10.1080/02786829408959748, 1995a.

Liu, P., P. J. Ziemann, D. B. Kittelson, and P. H. McMurry: Generating Particle Beams of Controlled Dimensions and Divergence: II. Experimental Evaluation of Particle Motion in Aerodynamic Lenses and Nozzle Expansions, *Aerosol Science and Technology*, *22*(3), 314-324, doi:10.1080/02786829408959749, 1995b.

Lopez-Hilfiker, F. D., C. Mohr, M. Ehn, F. Rubach, E. Kleist, J. Wildt, T. F. Mentel, A. Lutz, M. Hallquist, D. Worsnop, et al.: A novel method for online analysis of gas and particle composition: description and evaluation of a Filter Inlet for Gases and AEROsols (FIGAERO), *Atmospheric Measurement Techniques*, *7*(4), 983-1001, doi:DOI 10.5194/amt-7-983-2014, 2014.

Martinez, R. E., B. J. Williams, Y. Zhang, D. Hagan, M. Walker, N. M. Kreisberg, S. V. Hering, T. Hohaus, J. T. Jayne, and D. R. Worsnop: Development of a volatility and polarity separator (VAPS) for volatility- and polarity-resolved organic aerosol measurement, *Aerosol Science and Technology*, *50*(3), 255-271, doi:10.1080/02786826.2016.1147645, 2016.

Mensah, A. A., R. Holzinger, R. Otjes, A. Trimborn, T. F. Mentel, H. ten Brink, B. Henzing, and A. Kiendler-Scharr: Aerosol chemical composition at Cabauw, The Netherlands as observed in two intensive periods in May 2008 and March 2009, *Atmospheric Chemistry and Physics*, *12*(10), 4723-4742, doi:10.5194/acp-12-4723-2012, 2012.

Müller, M., T. Mikoviny, W. Jud, B. D'Anna, and A. Wisthaler: A new software tool for the analysis of high resolution PTR-TOF mass spectra, *Chemometrics and Intelligent Laboratory Systems*, *127*, 158-165, doi:10.1016/j.chemolab.2013.06.011, 2013.

Praplan, A. P., S. Schobesberger, F. Bianchi, M. P. Rissanen, M. Ehn, T. Jokinen, H. Junninen, A. Adamov, A. Amorim, J. Dommen, et al.: Elemental composition and clustering of α-pinene oxidation products for different oxidation conditions, *Atmospheric Chemistry and Physics Discussions*, *14*(22), 30799-30833, doi:10.5194/acpd-14-30799-2014, 2014.

Rohrer, F., B. Bohn, T. Brauers, D. Brüning, F. J. Johnen, A. Wahner, and J. Kleffmann: Characterisation of the photolytic HONO-source in the atmosphere simulation chamber SAPHIR, *Atmos. Chem. Phys.*, *5*(8), 2189-2201, doi:10.5194/acp-5-2189-2005, 2005.

Salvador, C. M., T. T. Ho, C. C. K. Chou, M. J. Chen, W. R. Huang, and S. H. Huang: Characterization of the organic matter in submicron urban aerosols using a Thermo-Desorption Proton-Transfer-Reaction Time-of-Flight Mass Spectrometer (TD-PTR-TOF-MS), *Atmospheric Environment*, *140*, 565-575, doi:10.1016/j.atmosenv.2016.06.029, 2016.

Seinfeld, J., and S. Pandis, ATMOSPHERIC CHEMISTRY AND PHYSICS: From Air Pollution to Climate Change, second edition, in *WILEY-INTERSCIENCE PUBLICATION*, edited, 2006.

Wiedensohler, A., W. Birmili, A. Nowak, A. Sonntag, K. Weinhold, M. Merkel, B. Wehner, T. Tuch, S. Pfeifer, M. Fiebig, et al.: Mobility particle size spectrometers: harmonization of technical standards and data structure to facilitate high quality long-term observations of atmospheric particle number size distributions, *Atmos. Meas. Tech.*, *5*(3), 657-685, doi:10.5194/amt-5-657-2012, 2012.

Williams, B. J., A. H. Goldstein, N. M. Kreisberg, and S. V. Hering: An In-Situ Instrument for Speciated Organic Composition of Atmospheric Aerosols:Thermal DesorptionAerosolGC/MS-FID (TAG), *Aerosol Science and Technology*, *40*(8), 627-638, doi:10.1080/02786820600754631, 2006.

Yu, J., D. R. Cocker, R. J. Griffin, R. C. Flagan, and J. H. Seinfeld: Gas-Phase Ozone Oxidation of Monoterpenes: Gaseous and Particulate Products, *Journal of Atmospheric Chemistry*, *34*(2), 207-258, doi:10.1023/a:1006254930583, 1999.

Zhao, Y., N. M. Kreisberg, D. R. Worton, A. P. Teng, S. V. Hering, and A. H. Goldstein: Development of an In SituThermal Desorption Gas Chromatography Instrument for Quantifying Atmospheric Semi-Volatile Organic Compounds, *Aerosol Science and Technology*, *47*(3), 258-266, doi:10.1080/02786826.2012.747673, 2013.

892 **Table 1: Experimental conditions for each experiment. For the tree emissions experiment there were two VOC injection periods.**

Experiment	Monoterpenes (ppb)	Ozone (ppb)	Duration (h)	Maximum SOA formed ($\mu g/m^3$)	SOA formation conditions	SOA aging Conditions
β-Pinene	120	700	34	130	Ozonolysis	Photochemical oxidation for 10 h
Limonene	25	150	17	50	Ozonolysis	Continuous NO_3 oxidation for 8 h
β-Pinene/Limonene mixture	60/12	300	26	60	Ozonolysis	Photochemical oxidation for 4 h
Tree emissions 1^{st} inj. / 2^{nd} inj.	65/10	300	30	80	Ozonolysis	Photochemical oxidation for 6 h

894

896

898

900

902

904

906

908

910

912

914

916 **Table 2: Instruments operating conditions.**

INSTRUMENT CHARACTERISTICS	ACM (in situ)	CHARON (online)	TD (in situ)
Time resolution (min)	240	1	120
Gas/particle separation	High vacuum	Denuder	Denuder and/or blank correction (filtered air)
Pre-concentration factor	21[a]	44	6000[b]
LOD[c] (ng/m^3)	35[d]	1.4[e]	0.02[b]
Temperature range (°C)	25 – 250	140	25 – 350
Heating rate (°C / min)	100	0	15
Temperature steps (°C)	100, 150, 250 (3 min)	none	None
Desorption pressure (atm)	1	< 1	1
Particle range (nm)	70 – 1000	70 – 1000	70 - 2000
PTR-ToF-MS model	8000	8000	8000
Drift tube Temperature (°C) / Pressure (mbar) / Voltage (V)	90 / 2.3 / 550	120 / 2.4 / 400 and 240	120 / 2.25 / 600
PTR-ToF-MS E/N (Td)	120	65 / 100	160
PTR-ToF-MS mass resolution (m/Δm)	2500	4500-5000	4000

[a] based on 240 min sampling at 80 mL/min and 3 min desorption at 300 mL/min

918 [b] based on 30 min sampling at 6 L/min and 3 min desorption at 10 mL/min a typical value for most ions based on the method in (Holzinger et al., 2010a)

920 [c] Limit of detection

[d] For signal on *m/z* 139 and 10 sec integration time

922 [e] For signals around *m/z* 200 and 1 min integration time

924

926

928

930

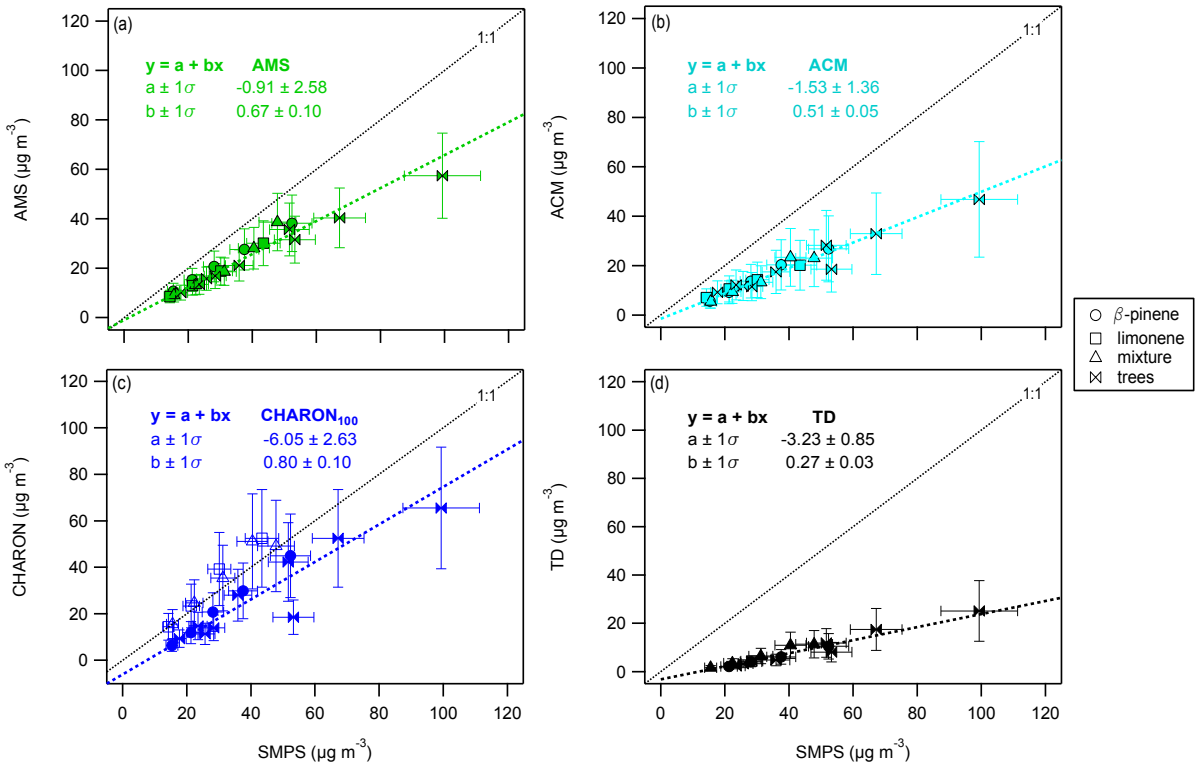

932 **Figure 1: Comparison of the organic mass concentration of (a) AMS (green), (b) ACM (ciel), (c) $CHARON_{100}$ (blue) and**
934 **(d) TD (black), to the SMPS (x-axis). Markers correspond to the different experiments with the mixture experiment**
936 **accounting for the mixture of β-pinene and limonene. AMS data presented are not corrected for collection efficiency.**
$CHARON_{100}$ corresponds to data taken only at 100 Td E/N operating condition. Error bars provide the uncertainty of
938 **each instrument (details in Section 2.3). A least orthogonal distance regression linear fit is applied for every instrument,**
taking into account all campaign measurement points. Exception is the CHARON limonene and mixture data (unfilled
markers) that were excluded due to experimental flaws. Details of the coefficient values and their standard deviation are
given on the upper left of each graph.

940

942

944

946

948

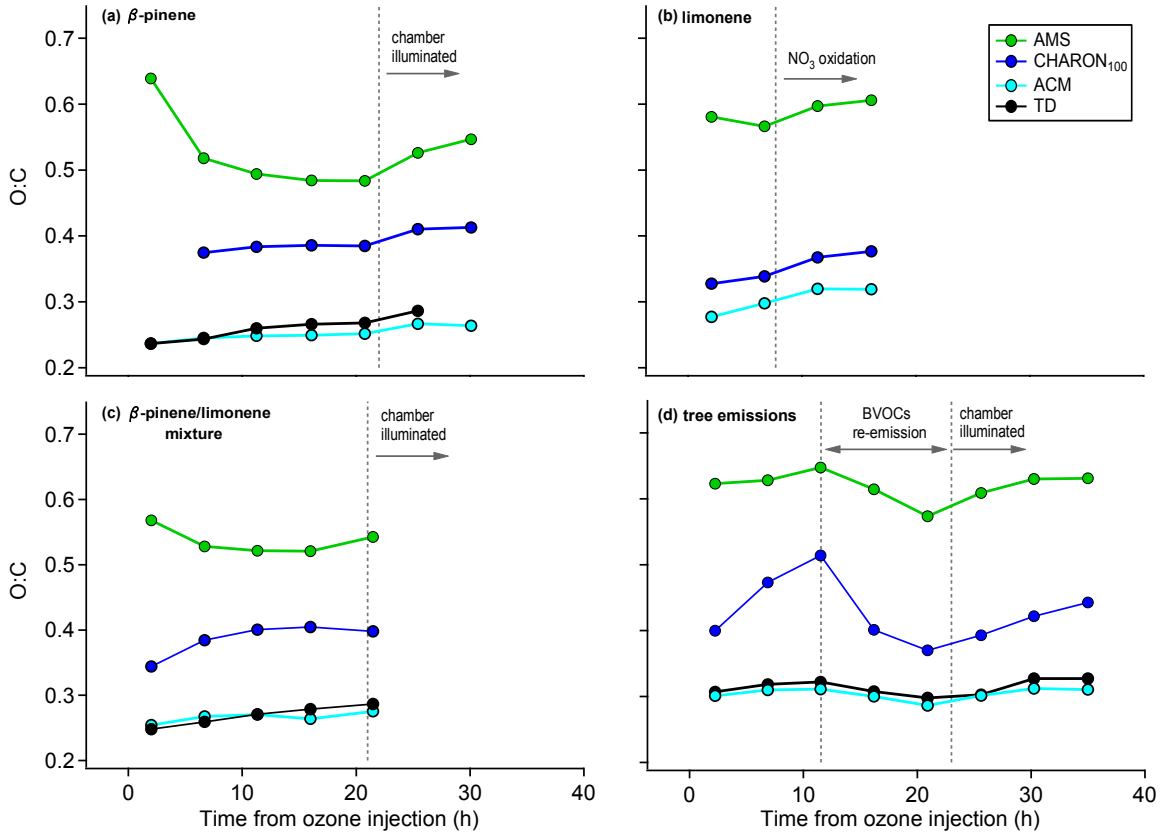

Figure 2: Bulk oxygen to carbon ratio comparison for the different instruments ($CHARON_{100}$: blue, AMS: green, ACM: ciel, TD: black) versus the time from ozone injection. Experimental description details are provided in Table 1.

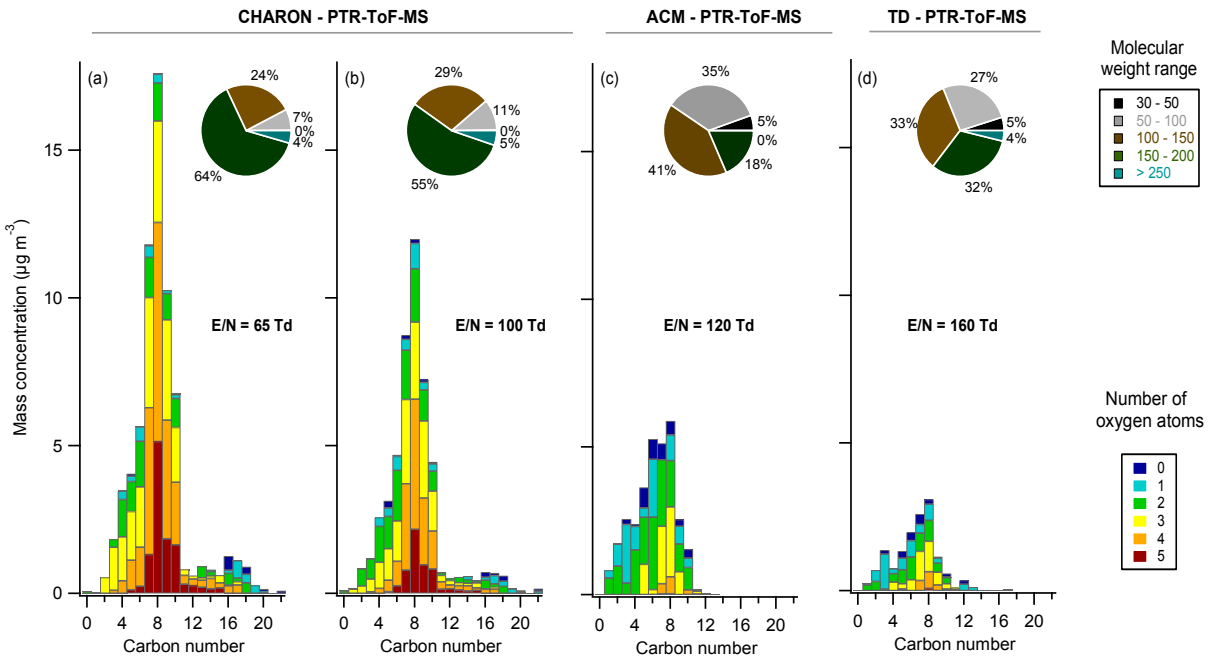

968 **Figure 3: OA mass concentration (y-axis) distributed based on the number of carbon atoms (x-axis). Bar colours**
970 **correspond to the contribution of oxygen atoms starting from 0 (blue) to 5 (red) for each carbon group when (a)**
CHARON was operated at E/N = 65 Td, (b) CHARON operated at 100 Td, (c) ACM operated at 120 Td and (d) TD
972 **operated at 160 Td. Pie charts correspond to the molecular weight contribution to the overall mass starting from *m/z* 30 –**
50 (black) up to *m/z* > 250 (ciel). Results shown in this graph are from the tree emissions experiment at a high OA mass
concentration, 25 h after the ozone injection (Figure 2 (d)).

974

976

978

980

982

984

986

988

990

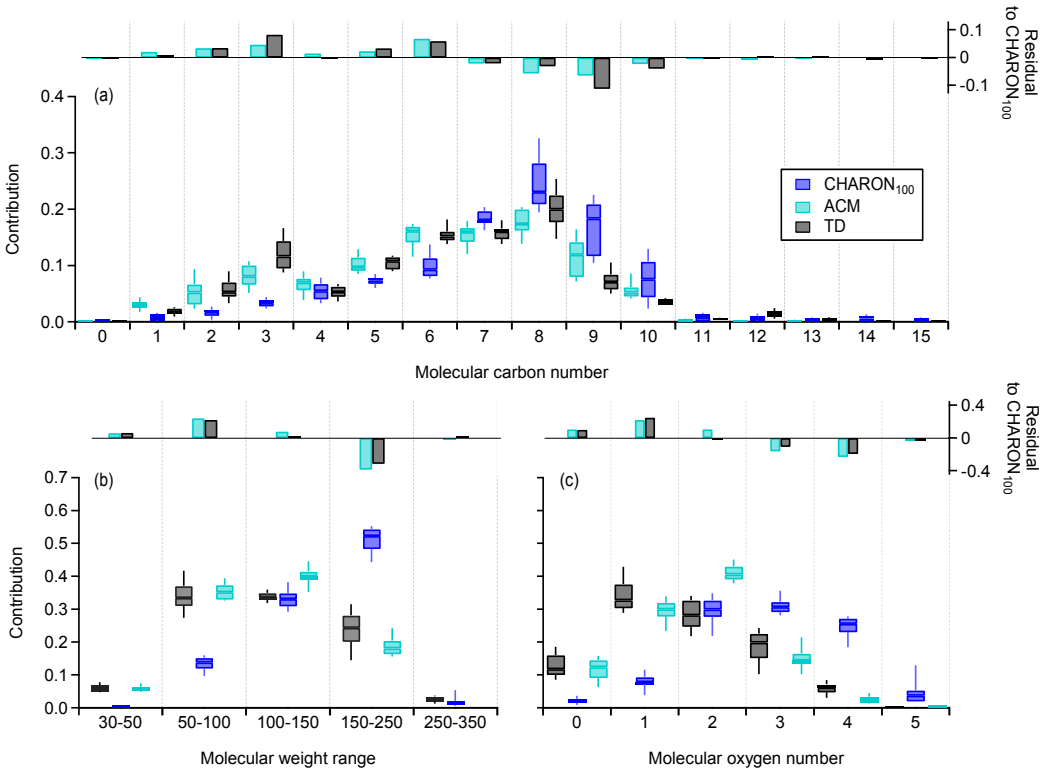

Figure 4: Box-and-whisker plots showing the relative OA mass concentration distribution dependent on (a) molecular carbon number, (b) molecular weight and (c) molecular oxygen number for the different instruments, indicated with different colours ($CHARON_{100}$ blue, ACM ciel and TD black). Each box-and-whisker corresponds to the median, 25th and 75th percentile levels of all data throughout the campaign. Upper graphs indicate the difference between the ACM and TD to the $CHARON_{100}$ median values defined as residual to $CHARON_{100}$.

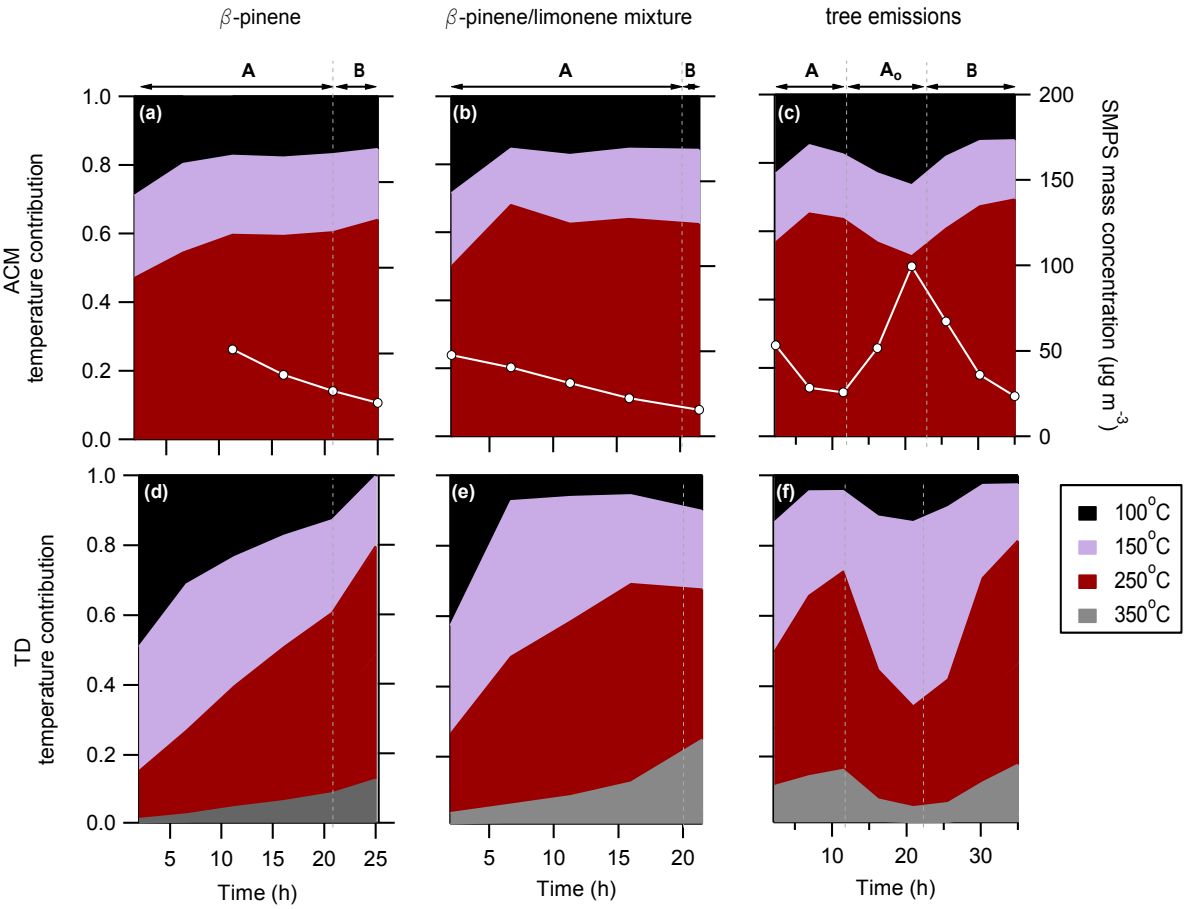

Figure 5: Temperature dependent mass concentration contribution (left y-axis) of ACM (upper plots: a, b, c) and TD (lower plots: d, e, f) for β-pinene (a, d), β-pinene and limonene mixture (b, e) and real tree emissions (c, f) versus the time since ozone injection (x-axis). White lines and circle markers (right y-axis) represent the SMPS mass concentration during each experiment. Dash vertical lines indicate the different experimental periods with A: the ozonolysis and SOA formation period, B: the chamber illumination and photo-oxidation period and A_0: the tree emissions BVOCs re-injection to the SAPHIR chamber.

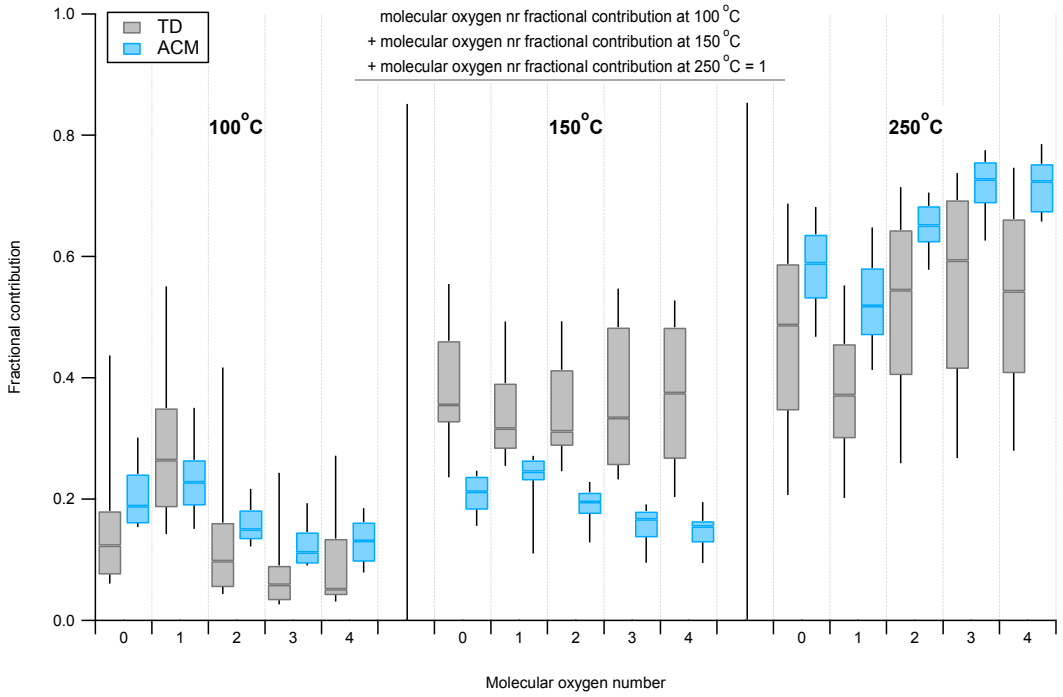

Figure 6: Box-and-whisker plots showing the distribution of the molecular oxygen number (x-axis), for the different temperature steps (100 °C, 150 °C, 250 °C) of ACM (ciel) and TD (black). Each box-and-whisker corresponds to the median, 25th and 75th percentile levels of all desorption points throughout the campaign. Upper equation indicates how the contribution of each molecular oxygen number, at each temperature, corresponds to unity.

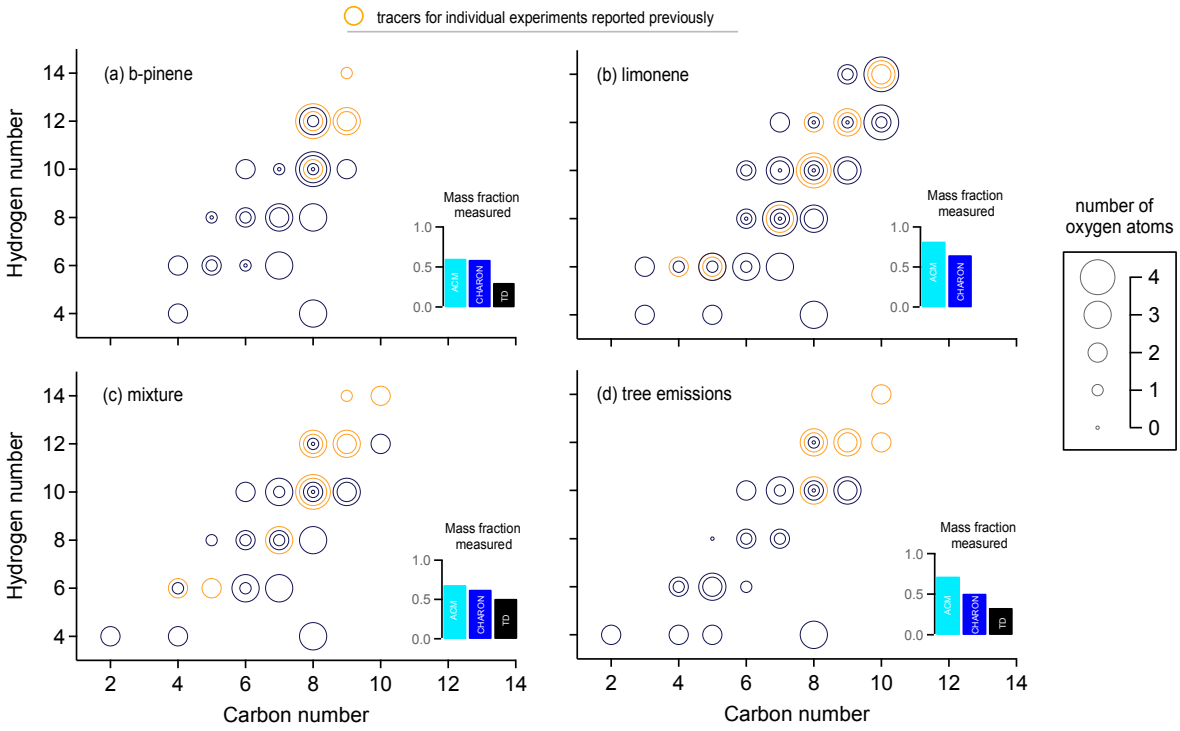

Figure 7: Chemical formula attribution based on the molecular carbon number (x-axis), hydrogen number (y-axis) and oxygen number (markers size) for (a) the ozonolysis of β-pinene, (b) ozonolysis and NO_3 oxidation of limonene, (c) ozonolysis of the β-pinene/limonene mixture and (d) ozonolysis of real tree emissions (Scotts pine). Markers correspond to compounds measured from all techniques (ACM, CHARON and TD) at high concentrations (within the 80 compounds observing highest concentration). Each circle corresponds to one compound. Orange markers indicate tracer compounds supported from previous publications (for details refer to Table S1). Bars indicate the fraction of mass explained when accounting only the presented compounds, for each instrument (ACM ciel, $CHARON_{100}$ blue and TD black) based on their total aerosol mass measured.